



1 **LongRunMIP – motivation and design for a large collection of**

2 **millennial-length AO-GCM simulations**

3 Maria Rugenstein*

4 *Institute for Atmospheric and Climate Science, ETH Zurich, CH-8092 Zurich, Switzerland*

5 *Max-Planck-Institute for Meteorology, Bundesstrasse 53, 20146 Hamburg, Germany*

6 Jonah Bloch-Johnson

7 *NCAS, University of Reading, Reading*

8 Ayako Abe-Ouchi

9 *Atmosphere and Ocean Research Institute, The University of Tokyo*

10 Timothy Andrews

11 *Met Office Hadley Centre, FitzRoy Road, Exeter, EX1 3PB*

12 Urs Beyerle

13 *Institute for Atmospheric and Climate Science, ETH Zurich, CH-8092 Zurich, Switzerland*

14 Long Cao

15 *School of Earth Sciences, Zhejiang University, Hang Zhou, Zhejiang Province, 310027, China*

16 Tarun Chadha

17 *ITS Research Informatics, ETH Zurich, Switzerland*

Early Online Release: This preliminary version has been accepted for publication in *Bulletin of the American Meteorological Society*, may be fully cited, and has been assigned DOI 10.1175/BAMS-D-19-0068.1. The final typeset copyedited article will replace the EOR at the above DOI when it is published.

18
19
20
21
22
23
24
25
26
27
28
29
30
31
32
33
34
35
36

Gokhan Danabasoglu

National Center for Atmospheric Research, P.O. Box 3000, Boulder, CO 80307

Jean-Louis Dufresne

*Centre National de la Recherche Scientifique, Université Pierre et Marie Curie, ENS, Ecole
Polytechnique, Paris, France*

Lei Duan

School of Earth Sciences, Zhejiang University, Hang Zhou, Zhejiang Province, 310027, China

Marie-Alice Foujols

Institut Pierre-Simon-Laplace, Sorbonne Université / CNRS, Paris, France

Thomas Frölicher

*Climate and Environmental Physics, Physics Institute, University of Bern, Switzerland,
Oeschger Centre for Climate Change Research, University of Bern, Switzerland*

Olivier Geoffroy

CNRM, Université de Toulouse, Météo-France, CNRS, Toulouse, France

Jonathan Gregory

*NCAS, University of Reading, Reading,
Met Office Hadley Centre, FitzRoy Road, Exeter, EX1 3PB*

Reto Knutti

Institute for Atmospheric and Climate Science, ETH Zurich, CH-8092 Zurich, Switzerland

37
38
39
40
41
42
43
44
45
46
47
48
49
50
51
52
53
54
55

Chao Li

Max-Planck-Institute for Meteorology, Bundesstrasse 53, 20146 Hamburg, Germany

Alice Marzocchi

National Oceanography Centre, European Way, Southampton, SO14 3ZH, UK

Thorsten Mauritsen

Stockholm University, SE-106 91 Stockholm, Sweden

Matthew Menary

LOCEAN, Sorbonne Université, Paris, France

Elisabeth Moyer

Department of the Geophysical Sciences, University of Chicago, Chicago, Illinois, USA

Larissa Nazarenko

NASA Goddard Institute for Space Studies, 2880 Broadway, New York, NY 10025

David Paynter

Geophysical Fluid Dynamics Laboratory, Princeton, New Jersey, USA

David Saint-Martin

CNRM, Université de Toulouse, Météo-France, CNRS, Toulouse, France

Gavin A. Schmidt

NASA Goddard Institute for Space Studies, 2880 Broadway, New York, NY 10025

Akitomo Yamamoto

56

Japan Agency for Marine-Earth Science and Technology, Yokohama, Japan

57

Shuting Yang

58

Danish Meteorological Institute, Lyngbyvej 100, DK-2100 Copenhagen, Denmark

59 *Corresponding author address: Maria Rugenstein, Max-Planck-Institute for Meteorology, Bun-

60 desstrasse 53, 20146 Hamburg, Germany

61 E-mail: maria.rugenstein@mpimet.mpg.de

ABSTRACT

62 We present a model intercomparison project, LongRunMIP, the first collec-
63 tion of millennial-length (1000+ year) simulations of complex coupled cli-
64 mate models with a representation of ocean, atmosphere, sea ice, and land
65 surface, and their interactions. Standard model simulations are generally only
66 a few hundred years long. However, modeling the long-term equilibration
67 in response to radiative forcing perturbation is important for understanding
68 many climate phenomena, such as the evolution of ocean circulation, time-
69 and temperature-dependent feedbacks, and the differentiation of forced signal
70 and internal variability. The aim of LongRunMIP is to facilitate research into
71 these questions by serving as an archive for simulations that capture as much
72 of this equilibration as possible. The only requirement to participate in Lon-
73 gRunMIP is to contribute a simulation with elevated, constant CO₂ forcing
74 that lasts at least 1000 years. LongRunMIP is a MIP of opportunity in that
75 the simulations were mostly performed prior to the conception of the archive
76 without an agreed-upon set of experiments. For most models, the archive
77 contains a preindustrial control simulation and simulations with an idealized
78 (typically abrupt) CO₂ forcing. We collect 2D surface and top-of-atmosphere
79 fields, and 3D ocean temperature and salinity fields. Here, we document the
80 collection of simulations and discuss initial results, including the evolution of
81 surface and deep ocean temperature and cloud radiative effects. As of sum-
82 mer 2019, the collection includes 50 simulations of 15 models by 10 modeling
83 centers. The data of LongRunMIP are publicly available. We encourage sub-
84 mission of more simulations in the future.

85 (Capsule Summary) LongRunMIP is the first collection of millennial-length simulations of com-
86 plex coupled climate models and enables investigations of how these models equilibrate in re-
87 sponse to radiative perturbations.

88 **1. Motivation and objectives**

89 Millennial-length climate simulations are necessary to understand the equilibrium states that oc-
90 cur in response to external forcings, as well as the relationship between transient and equilibrated
91 behavior. Unforced millennial-length simulations are useful as well, as they allow us to consider
92 long-term internal variability and to analyze shorter-term variability with increased statistical cer-
93 tainty. Reasons to study these long time scales include:

- 94 • To better understand long-term climate dynamics. Outstanding issues include the time scales
95 of ocean circulation response (e.g., Jansen et al. 2018; Rind et al. 2018), continental drying
96 trends (e.g., Sniderman et al. 2019) or sea level rise (e.g., Bilbao et al. 2015; Rugenstein et al.
97 2016c).

- 98 • To help predict the impacts of 20th and 21st century emissions on century timescales, such as
99 ice sheet stability, deep ocean warming, or polar amplification (e.g., Frölicher and Joos 2010;
100 Clark et al. 2016; Mauritsen and Pincus 2017), which are rarely explicitly simulated using a
101 fully-coupled climate model.

- 102 • To more accurately estimate Equilibrium Climate Sensitivity (ECS), which is the equilibrium
103 response of the surface air temperature to a doubling of CO₂ due to the “fast” feedbacks water
104 vapor, lapse rate, clouds, and sea ice but excluding Earth system feedbacks such as changes
105 in the carbon cycle, ice sheets, or vegetation. While ECS has long been a focus of scientific

106 inquiry, substantial uncertainty remains as to its value (e.g., Charney et al. 1979; Knutti et al.
107 2017).

- 108 ● To understand the relationship between the transient response of the climate and its equilibra-
109 tion. Since radiative feedbacks can depend on the evolution of the spatial pattern of warming
110 (e.g., Senior and Mitchell 2000; Winton et al. 2010; Armour et al. 2013; Andrews et al. 2015;
111 Andrews and Webb 2018) and on the background temperature (e.g., Colman and McAvaney
112 2009; Caballero and Huber 2013; Block and Mauritsen 2013; Meraner et al. 2013; Bloch-
113 Johnson et al. 2015), a constant effective sensitivity of the climate is an inadequate assump-
114 tion. Several methods have been proposed to predict the equilibrium response from transient
115 simulations given a changing global feedback (Held et al. 2010; Winton et al. 2010; Armour
116 et al. 2013; Geoffroy et al. 2013b,a; Frölicher et al. 2014; Proistosescu and Huybers 2017;
117 Saint-Martin et al. 2019), but only fully equilibrated climate model simulations can serve to
118 test how well these methods predict equilibrium conditions.
- 119 ● To test theories for the relationship between feedbacks at different time-scales (Gregory et al.
120 2015, 2016; Zhou et al. 2016; Rugenstein et al. 2016a; Armour 2017; Proistosescu and Huy-
121 bers 2017; Ceppi and Gregory 2017; Andrews and Webb 2018; Andrews et al. 2018), and
122 to quantify the influence of slow, centennial-scale modes on the temperature evolution of the
123 last century (Armour 2017; Proistosescu and Huybers 2017).
- 124 ● To understand the relevance, time scales, and magnitude of the energy imbalances and drifts
125 exhibited by climate models (e.g., Hobbs et al. 2016), with the potential application of de-
126 creasing the spin-up time needed to run these models.
- 127 ● To understand the relationship between the forced response and internal variability. This re-
128 lationship is currently studied using the time frame of one or two centuries, which is not

129 enough to robustly quantify the internal variability under consideration (e.g., Maher et al.
130 2018; Lutsko and Takahashi 2018; Bloch-Johnson et al. in revision), millennial time scales
131 with varying forcings (e.g., Köhler et al. 2017; Khon et al. 2018; Rehfeld et al. 2018) or by
132 using expensive large ensemble simulations on decadal to centennial time scales (e.g., Deser
133 et al. 2012; Maher et al. 2019; Rodgers et al. 2015). Millennial long simulations allow us to
134 differentiate the transient response from the equilibrated forced response, even for quantities
135 with large internal variability, such as precipitation, droughts, or the El Niño-Southern Os-
136 cillation (ENSO), and also the significance of a change in internal variability in a transient
137 simulation relative to the control simulation (e.g., Brown et al. 2017).

- 138 • To compare climate model responses and paleo proxies, e.g. of surface or deep ocean temper-
139 atures or hydrological conditions on land in order to provide an independent way of testing
140 climate models (Gebbie and Huybers 2019; Burls and Fedorov 2017; Scheff et al. 2017).

141 With LongRunMIP, we aim to advance knowledge in the above mentioned areas, fill a gap in the
142 CMIP protocols (Taylor et al. 2011; Eyring et al. 2016), and collect published data in one location
143 for easy public access.

144 **The goals of LongRunMIP are**

- 145 a) to continuously gather existing millennial-length simulations (both published and unpub-
146 lished)
- 147 b) to standardize the collected data (e.g., using the same units and sign conventions)
- 148 c) to make the data publicly available and easily accessible
- 149 d) to foster an interdisciplinary community of users working on millennial-length problems,
150 with experts on oceanography, atmospheric dynamics, energy balance modeling, ice sheet
151 modeling, and paleoclimatology

152 **The objectives of this paper** are to

- 153 a) motivate the data collection strategy (Section 2)
- 154 b) specify the requirements for LongRunMIP contributors (Section 2 and b)
- 155 c) give an overview of currently submitted simulations and models (Section 2a, b, and Table 1)
- 156 d) give a sample of some initial analysis on these simulations (Section 3)
- 157 e) show how LongRunMIP relates to the existing literature on millennial-length simulations
158 (Section 4a)
- 159 f) discuss the limitations and opportunities of LongRunMIP (Section 4b and c).

160 **2. Experimental design and data collection strategy**

161 LongRunMIP is the first and largest compilation of millennial-length simulations of complex cli-
162 mate models to date, where a “complex climate model” is understood to include an atmospheric,
163 sea ice, land, and full depth ocean component, i.e. Atmosphere-Ocean General Circulation Mod-
164 els (AO-GCMs) with a dynamic atmosphere and ocean, as opposed to Models of Intermediate
165 Complexity (EMICs), which are often used to study millennial-length questions in climate science
166 (e.g., Zickfeld et al. 2013; Levermann et al. 2013). These model simulations include the “fast”
167 feedbacks, such as changes in water vapor, lapse rate, sea ice, and clouds (Charney et al. 1979),
168 but no “slow” feedbacks, such as changes in the ice-sheets. Vegetation is treated differently in the
169 models (see Section 2b). In Section 4 we discuss the implications and limitations of our approach.
170 Our goal is to collect as many simulations from as many independent models as possible, while
171 keeping the archive and data sharing manageable. Consequently, we keep our requirements for
172 contributions low.

173 *a. Simulations and variables*

174 A step-increase in atmospheric CO₂ concentrations (in the following called “step-forcing”) is
175 one of the simplest experiments for studying a model’s response to forcing and is used as a bench-
176 mark simulation in CMIP3, CMIP5, and CMIP6 (Meehl et al. 2007; Taylor et al. 2011; Eyring
177 et al. 2016). More realistic, gradual forcing scenarios have been shown to be representable by the
178 step-forcing scenarios and exhibit feedbacks that correlate with those computed from step-forcing
179 simulations (Good et al. 2013, 2015; Geoffroy and Saint-Martin 2014; Colman and Hanson 2016).
180 The CMIP3 protocol required a step-forcing of *doubling* atmospheric CO₂ (here referred to as
181 *abrupt2x*) above pre-industrial levels in a slab (i.e. non-dynamical) ocean, which for decades has
182 been used to define ECS (e.g., Charney et al. 1979; Boer and Yu 2003c; Danabasoglu and Gent
183 2009). The integration time scale of these model setups are a couple of decades. However, a
184 *quadrupling* of CO₂ (here referred to as *abrupt4x*) above pre-industrial levels has a better ratio of
185 forced signal to internal variability. Because the forced response was assumed to scale linearly
186 with increased forcing, the CMIP5 protocol requested an abrupt quadrupling of CO₂, now in a
187 fully coupled model with a dynamical ocean, requiring longer integration time scales. The CMIP6
188 protocol again requests abrupt CO₂ quadrupling experiments, but encourages also the submission
189 of abrupt CO₂ doublings, to study the relation between different forcing levels (Eyring et al. 2016;
190 Good et al. 2016). CMIP5 and 6 protocols require the submission of 150 years of model output.
191 A representative response of surface temperature anomalies and top of the atmosphere (TOA) ra-
192 diative imbalance to an *abrupt4x* scenario is shown in Fig. 1. All anomalies mentioned in this
193 paper are computed as the difference of the experiment from the average of the control simulation.
194 After the 150 years of CMIP protocol length (blue shading) and after 1000 years (the minimum
195 contribution to LongRunMIP, light red shading), the surface temperature response of the exem-

196 plary model shown here has reached 75 % and 88 % of its final value respectively, while the TOA
197 radiation has equilibrated 85 % and 93 % of the forcing respectively (7.6 W m^{-2} for this model).
198 Thus, the final equilibration is a CPU-intensive exercise; the model shown here needs 4000 years
199 to balance the final 0.5 W m^{-2} (dark red shading).

200 The set of variables we collect is motivated by the interest of the LongRunMIP contributors and
201 organizers in ECS, temperature and time dependent feedbacks, and deep ocean warming. Table
202 1 lists the variable names, units, and temporal and spatial resolution of the requested variables.
203 The naming and sign conventions follow the CMIP5 protocol¹. Given the large amount of data
204 involved, we have kept our requested variable list low to allow as many groups as possible to
205 participate. For the same reason, we do not request the data to be “CMORized”², i.e. written in
206 conformance with the CMIP standards. However, we do homogenize signs, variable long names,
207 and units, and also provide a regridded version of the fields, as well as global means.

208 *b. Minimal, optimal, and current contributions*

209 The *minimal requirement* to contribute to LongRunMIP are annual fields of a single simulation
210 of any CO_2 forcing scenario that has at least 1000 years of constant forcing, along with a control
211 simulation of any length. The complexity of the model should be CMIP5-class and include dy-
212 namic atmosphere, ocean, and sea ice components. An *optimal contribution* comprises monthly
213 fields of fully equilibrated *abrupt2x*, *4x*, and *8x* simulations and a control simulation of several
214 millennia.

215 Table 2 lists the model characteristics of the current contributions. Because the archive is assem-
216 bled from experiments initiated independently for research purposes by multiple modeling groups,
217 there is no pre-defined protocol like for the CMIP simulations. The models are diverse in origin

¹http://cmip-pcmdi.llnl.gov/cmip5/data_description.html

²<https://pcmdi.llnl.gov/CMIP6/Guide/dataUsers.html>

218 and sample the CMIP5 range of models well (see discussion on model genealogy in Knutti 2010).
219 Table 2 lists references for each model and publications using (parts of) the model output. Most
220 of the current contributions to LongRunMIP are extensions of CMIP5 simulations, sometimes
221 with updated model versions, while one model is an extension of a CMIP3 and another model an
222 extension of a CMIP6 contributions (CCSM3 and CNRM-CM6-1 respectively).

223 Many of our current contributions fall short of the optimal expectation for equilibrium, because
224 even several millennia are insufficient for the deep ocean to equilibrate (see discussion around
225 Fig. 4). However, a few millennia appear to be enough for the surface temperature and TOA
226 radiative imbalance to reach a new steady state in most models (see Section 3), and many questions
227 can be adequately addressed with the current contributions. Our approach is to be inclusive, and
228 to leave it to the user to determine the degree of equilibration needed for their research and to
229 develop criteria for model selection.

230 Most contributions are step-forcing simulations, generally to 2x or 4x pre-industrial CO₂ con-
231 centrations (in Fig. 2 *abrupt2x* colored in yellow, *abrupt4x* in orange, *abrupt8x* in dark red;
232 *abrupt2.4x* and *abrupt4.8x* in dark and light pink). There are currently three exceptions: 1) some
233 model simulations have gradual increases in CO₂ at 1% per year until doubled or quadrupled con-
234 centrations are reached, after which the concentration is kept constant (*1pct2x* and *1pct4x*, light
235 and medium red in Fig. 2). 2) One model simulates the 1850-2010 period, after which CO₂ in-
236 creases either piecewise linearly for 90 years until reaching 2.4x pre-industrial values (CCSM3II).
237 3) Finally, one model simulates the historical period and then the CMIP5 extended representative
238 concentration pathway 8.5 (including CH₄, N₂O, CFC11, and CFC12 in addition to CO₂) until
239 year 2300 after which all forcing agents are kept constant (*RCP8.5+*, violet in Fig. 2)

240 For the models that did not contribute a a millennial-long step-forcing simulation, we collect
241 short (typically 150 year) step-forcing simulations, generally from the CMIP5 archive. These

242 simulations can be used to estimate the effective climate sensitivity and to relate transient and
243 equilibrium responses. They are not mentioned in Table 2 and Fig. 2.

244 Most contributors were able to submit all requested variables. Some models only stored annual
245 output, while for a few models the entire model output (including many more variables than listed
246 in Table 1) is available. In principle, but with considerable effort, additional variables not listed in
247 Table 1 could be requested from some or all contributors.

248 Some models are outliers in some sense. For example, the simulation *abrupt4x* of FAMOUS
249 warms anomalously strong (Fig. 2 and 7) due to a shortwave cloud effect which is positive through-
250 out the simulation and longwave clear-sky effect, which increases anomalously strongly (not
251 shown, see Rugenstein et al. (2019)). In principle though, such extreme behavior could represent
252 possible characteristics of the real world (e.g., Bloch-Johnson et al. 2015; Schneider et al. 2019).
253 Another atypical model is EC-Earth-PISM, which is the only model with an interactive Greenland
254 ice sheet. This additional component and its historical and RCP8.5+ forcing scenario makes it
255 harder to compare the simulation to other models and attribute changes to one forcing component.
256 This model also does not equilibrate but finally produces a negative TOA imbalance, which prob-
257 ably would increase if the simulation was integrated further. We encourage similar “problematic”
258 submissions, since our focus is on understanding model behavior and the large range of model
259 responses (discussed in Section 3).

260 In nine models, the vegetation is fixed to pre-industrial conditions (ECHAM5, CCSM3,
261 CCSM3II, HadCM3L, FAMOUS, MIROC32, ECEARTH, GISSE2R, CNRMCM61), while the
262 other seven models have dynamic vegetation schemes (MPIESM11, MPIESM12, CESM104,
263 HadGEM2, GFDLESM2M, GFDLCM3, IPSLCM5A).

264 **3. Sample of model output**

265 *a. Imbalances in the control simulation and drift*

266 In principle, the TOA radiative imbalance should be zero in a control simulation. Most models
267 contributing to LongRunMIP do not loose or gain energy (Fig. 3). However, some models that are
268 equilibrated in the sense that they show no substantial drift, still have a constant energy leakage.
269 For CMIP5 models, imbalances of the same order of magnitude (and larger) have been shown to be
270 uncorrelated with the forced response (Hobbs et al. 2016). If computing atmospheric anomalies,
271 we suggest users to take the difference of each time step to the time-averaged control simulation
272 imbalance, except for CCSM3II and GFDL-CM3 for which the difference to a polynomial fit to
273 the control simulation time series seems appropriate (see Fig. 3).

274 The deep ocean (defined here as depth level around 2 km) has an astonishingly small drift in
275 the global average in most models (Fig. 4, lowest panel). While the surface ocean time scales
276 closely follows the global mean surface air temperature anomaly, the deep ocean takes centuries
277 to equilibrate. Panel a and b of Fig. 4 display the surface and deep ocean temperature anomalies,
278 computed as the difference of the forced and control simulations, while the lowest panel shows the
279 absolute temperatures of the deep ocean in the control simulations to indicate the model spread in
280 the base state. Previous work on long-term trends in deep ocean temperature and salinity shows
281 that these trends may reflect ongoing changes in stratification and the strength and depth of the
282 Atlantic Meridional Overturning Circulation (AMOC; e.g., Stouffer and Manabe 2003; Rugenstein
283 et al. 2016a; Marzocchi and Jansen 2017; Jansen et al. 2018). Even if the energy flux imbalance
284 at the TOA or the ocean surface are close to a new steady state this does not necessarily indicate
285 that the deep ocean is equilibrated as well (Zhang et al. 2013; Hobbs et al. 2016; Marzocchi and
286 Jansen 2017). Reaching deep ocean equilibration may not be necessary for studies concerned with

287 surface properties only. However, for interpretation of paleo proxies and comparison with model
288 simulations, distinguishing between the transient and equilibrium response in the intermediate or
289 deep ocean is necessary (Zhang et al. 2013; Marzocchi and Jansen 2017; Rind et al. 2018; Jansen
290 et al. 2018).

291 *b. Evolution of surface temperature and cloud radiative effect*

292 The evolution of large scale surface air temperature patterns on decadal to millennial time scales
293 (Fig. 5) are robust among models and different forcing levels. The simulations show a strong
294 land-sea warming contrast on short time scales and little warming over the Southern Ocean on
295 decadal to centennial time scales (e.g., Manabe et al. 1991; Gregory 2000; Joshi and Gregory
296 2008; Geoffroy and Saint-Martin 2014; Armour et al. 2016). A warming pattern reminiscent of
297 the positive phase of ENSO and the Interdecadal Pacific Oscillation occurs throughout the Pacific
298 basin (panel b; Held et al. 2010; Song and Zhang 2014; Andrews et al. 2015; Luo et al. 2017)
299 but decays on centennial to millennial time scales (panel c and d), with a large model spread in
300 time scales (not shown). As it approaches equilibrium, the temperature pattern becomes more
301 homogeneous, the land-sea warming contrast reduces (e.g., Held et al. 2010; Geoffroy and Saint-
302 Martin 2014), and the Southern Hemisphere high latitudes keep warming beyond year 1000. As
303 in previous studies, the AMOC first declines (Gregory et al. 2005; Zhu et al. 2014; Kostov et al.
304 2014; Trossman et al. 2016) and then recovers (Stouffer and Manabe 2003; Li et al. 2013; Zickfeld
305 et al. 2013; Rugenstein et al. 2016a; Rind et al. 2018), resulting in a delayed warming in the North
306 Atlantic. Panel a, b, and e correspond to the blue shading in Fig. 1, and are known from CMIP5
307 simulations (e.g., Andrews et al. 2015), while panel c, d, f, and g highlight that the simulations still
308 warm substantially on centennial to millennial time scales, mainly in areas with more sensitive –
309 i.e. positive or small negative – feedbacks (Rugenstein et al. 2019).

310 Normalizing the zonal-mean temperature anomaly by the global mean warming reveals the rel-
311 ative zonal-mean warming (Fig. 6). Arctic amplification begins very early in the simulations and
312 warming throughout the Southern Hemisphere is lower than the global average in almost all mod-
313 els for the first centuries. Between year 100 and 1000 the Southern Hemisphere warms more than
314 the Northern Hemisphere in all latitudes poleward from 30°, in some regions by more than 4 K.
315 Antarctic warming slowly increases, but is still substantially less than Arctic amplification (e.g.,
316 Salzmänn 2017). In a couple of models, the amplitude of Antarctic and Arctic amplification is
317 the same after 4000 years of model integration time (GISSE2R and ECHAM5; Li et al. 2013),
318 while in other models the Antarctic amplification stays substantially smaller and still increasing
319 after a couple of thousand years. LongRunMIP shows that there is no reduction in model spread
320 in the polar regions through time and that although all models follow a similar large scale pattern
321 evolution (Fig. 5), the local response time scales, e.g. in the North Atlantic, Southern Ocean, or
322 equatorial Pacific differ by hundreds to thousands years.

323 While the large scale temperature response is rather robust between models and simulations,
324 the cloud radiative effect (CRE) differs strongly in magnitude and time evolution, both between
325 models and between forcing levels for the same model (Fig 7). We show the shortwave CRE –
326 computed as the difference between “all sky” and “clear sky” shortwave radiative fluxes (e.g.,
327 Ramanathan et al. 1989; Ceppi et al. 2017) – as a function of surface air temperature anomaly.
328 The models disagree in the overall sign, as expected from CMIP5 models on shorter time scales
329 (e.g., Vial et al. 2013; Caldwell et al. 2015), but can even change sign within a single simulation
330 (e.g., ECEARTH or CESM *abrupt8x*). The strength of variation in time within one simulation
331 can depend strongly on the forcing level (e.g. MIROC32 *1pct2x* vs. *1pct4x*) and the time scales
332 of change differ between the models (e.g. IPSLCM5R vs. MPIESM12 *abrupt4x*). For some

333 simulations, cloud response barely changes with temperature, contributing negligibly to the overall
334 feedback (e.g. MPIESM12 *abrupt16x*, CESM104 *abrupt4x*, and MIROC32 *1pct2x*).

335 **4. Discussion and Outlook**

336 *a. Published millennial-length simulations*

337 Models of intermediate complexity are the most common tools used to study century to millen-
338 nium time scales in the climate system (e.g., Zickfeld et al. 2013; Eby et al. 2013; Levermann et al.
339 2013; Rugenstein et al. 2016c; Jansen et al. 2018). However, they usually have a poorly resolved
340 atmosphere and little or no representation of cloud processes. In contrast, the publications in Table
341 3 feature millennium-length AO-GCM simulations. Asterisks mark contributions to LongRunMIP.
342 These papers provide a solid body of work on millennial-length climate simulations, but rarely use
343 the same forcing levels and simulation length and focus on different aspects of the climate sys-
344 tem. Three papers compare model formulation and processes of two AO-GCMs each (Frölicher
345 et al. 2014; Paynter et al. 2018; Krasting et al. 2018), but otherwise models have not been sys-
346 tematically compared against each other. Fig. 4 and 7 show that AO-GCMs can strongly differ in
347 their behavior. Spatial patterns of e.g., precipitation and surface heat fluxes also vary strongly be-
348 tween models and between different forcing scenarios for the same model (not shown), suggesting
349 that some mechanisms and processes discussed in the published literature are not generalizable
350 across models. For example, there is disagreement about which regions are thought to dominate
351 the changing feedback parameter (Senior and Mitchell 2000; Andrews et al. 2015; Meraner et al.
352 2013; Caballero and Huber 2013) or whether or not, and on which time scales, the AMOC recovers
353 from its initial reduction (Voss and Mikolajewicz 2001; Stouffer and Manabe 2003; Li et al. 2013;
354 Rind et al. 2018; Thomas and Fedorov 2019). Paleo climate simulations are often several thou-

355 sand years long, however, they usually include boundary conditions such as ice sheets or changing
356 continental configurations, which differ from the ones used here. However, paleo climate studies
357 often discuss equilibration time scales and deep ocean temperature trends relevant to the types
358 of models included in LongRunMIP (e.g., Brandefelt and Otto-Bliesner 2009; Zhang et al. 2013;
359 Klockmann et al. 2016; Marzocchi and Jansen 2017; Gottschalk et al. 2019).

360 *b. Limitations*

361 LongRunMIP analyses are currently limited mainly by the collected *variables* (Table 1). In-
362 cluding cloud fields and 3D atmospheric temperature and humidity fields, for example, would
363 allow users to study atmospheric dynamics and radiative feedbacks in more detail. The *differ-*
364 *ent forcing scenarios* of model contributions to LongRunMIP are both a strength and weakness.
365 Minimal requirements have encouraged a large number of contributions so far. However, study-
366 ing a single forcing scenario requires model selection or scaling between different forcing levels.
367 *Slab ocean simulations*, which replace a model's dynamical ocean with a much shallower non-
368 dynamical mixed-layer, are a computationally cheap tool to compare fast and slow time scales and
369 the relevance of surface warming patterns (Boer and Yu 2003c; Danabasoglu and Gent 2009; Li
370 et al. 2013). We hope to receive submissions of these simulations in the future, to allow analysis of
371 their utility. Century to millennial-time scales in the real world include more processes and *Earth*
372 *System Feedbacks* than are included in LongRunMIP simulations, such as the carbon cycle, vege-
373 tation feedbacks, forcing agents other than CO₂ (such as other greenhouse gases or aerosols), ice
374 sheets, glacial rebound effects, changes to continental configuration, and orbital variation. Further,
375 the real climate system is never in equilibrium or steady state, because the forcing continuously
376 changes (e.g., Köhler et al. 2017). These Earth system feedbacks and additional forcings must be

377 taken into account when comparing the LongRunMIP models with paleo proxies or when project-
378 ing or predicting changes in future centuries or millennia.

379 *c. Summary and expected impact*

380 LongRunMIP is the first archive of millennial-length simulations of complex climate models,
381 featuring 50 simulations of 15 models by 10 modeling centers under various forcing scenarios (Ta-
382 ble 2). The archive provides an unprecedented opportunity to study the equilibrium response of a
383 large number of models to forcing. The variables included allow study of a range of phenomena
384 associated with the atmosphere, ocean, land, and sea ice (Table 1), and we expect LongRunMIP to
385 contribute to current discussions laid out in Section 1. This includes ocean heat uptake, sea level
386 rise, ocean circulation response to warming, large scale modes of variability, sea ice reduction,
387 polar amplification, precipitation variability, atmospheric dynamics, long-term memory in time
388 series, spatial warming patterns, ocean - atmosphere interactions, model spin-up techniques, the
389 relation of internal variability and forced response under different forcing levels, committed cli-
390 mate response, and the relation of time and state dependence of fast feedbacks and Earth System
391 Feedbacks and processes.

392 LongRunMIP is a MIP of opportunity, without an agreed upon protocol, and is a result of the
393 willingness of individual research groups to provide model output from simulations often con-
394 ducted over years of real-world time. As a result, the experiments are not standardized, but most
395 models provided a millennial-length simulation that begins with an abrupt quadrupling of CO₂
396 concentration. In addition to collecting simulations, we provide output with standardized formats
397 and variable names, and include versions regridded to a common grid, as well as global averages.

398 LongRunMIP builds upon a body of pioneering studies that looked at the behavior of models be-
399 yond the centennial scale (Table 3), LongRunMIP allows this sort of analysis to be applied across

400 a diverse group of models that exhibit strikingly different behavior (Fig. 7), and hopefully encour-
401 age others to look beyond the limitations and assumptions normally imposed by computational
402 constraints, to directly study the equilibration of the fully coupled atmosphere-ocean system.

403 *Data access and sharing*

404 LongRunMIP currently consists of 15 TB of data and available for download at
405 <https://data.iac.ethz.ch/longrunmip/>. Fields shown in this paper can be accessed on
406 <https://data.iac.ethz.ch/longrunmip/BAMS/>.

407 See www.longrunmip.org for more details on available variables, contact information, sample
408 figures and videos, and links to join a discussion community. We will be collecting more
409 simulations over the next couple of years.

410 *Acknowledgments.* NCAR is sponsored by the US National Science Foundation. TA was sup-
411 ported by the Joint UK BEIS/Defra Met Office Hadley Centre Climate Programme (GA01101).
412 NCAR is a major facility sponsored by the US National Science Foundation under Cooperative
413 Agreement No. 1852977 TLF acknowledges support from the Swiss National Science Foundation
414 under grant PP00P2_170687, from the EU-H2020 project CCiCC, and from the Swiss National
415 Supercomputing Centre (CSCS). CL was supported through the Clusters of Excellence CliSAP
416 (EXC177) and CLICCS (EXC2037), University Hamburg, funded through the German Research
417 Foundation (DFG). SY was partly supported by European Research Council under the European
418 Community's Seventh Framework Programme (FP7/20072013)/ERC grant agreement 610055 as
419 part of the ice2ice project. This work was made possible for IPSL thanks to the HPC resources
420 of TGCC and IDRIS made available by GENCI (Grand Equipement National de Calcul Inten-

421 sif), CEA (Commissariat à l’Energie Atomique et aux Energies Alternatives) and CNRS (Centre
422 National de la Recherche Scientifique) (project 016178).

423 **References**

424 Andrews, T., J. M. Gregory, and M. J. Webb, 2015: The dependence of radiative forcing and
425 feedback on evolving patterns of surface temperature change in climate models. *Journal of*
426 *Climate*, **28** (4), 1630–1648, URL <http://dx.doi.org/10.1175/JCLI-D-14-00545.1>.

427 Andrews, T., and M. J. Webb, 2018: The Dependence of Global Cloud and Lapse Rate Feedbacks
428 on the Spatial Structure of Tropical Pacific Warming. *Journal of Climate*, **31** (2), 641–654,
429 doi:10.1175/JCLI-D-17-0087.1, URL <https://doi.org/10.1175/JCLI-D-17-0087.1>.

430 Andrews, T., and Coauthors, 2018: Accounting for Changing Temperature Patterns Increases
431 Historical Estimates of Climate Sensitivity. *Geophysical Research Letters*, **45** (16), 8490–
432 8499, doi:10.1029/2018GL078887, URL [https://agupubs.onlinelibrary.wiley.com/doi/abs/10.](https://agupubs.onlinelibrary.wiley.com/doi/abs/10.1029/2018GL078887)
433 [1029/2018GL078887](https://agupubs.onlinelibrary.wiley.com/doi/abs/10.1029/2018GL078887).

434 Armour, K. C., 2017: Energy budget constraints on climate sensitivity in light of inconstant
435 climate feedbacks. *Nature Climate Change*, **7**, 331 EP –, URL [http://dx.doi.org/10.1038/](http://dx.doi.org/10.1038/nclimate3278)
436 [nclimate3278](http://dx.doi.org/10.1038/nclimate3278).

437 Armour, K. C., C. M. Bitz, and G. H. Roe, 2013: Time-Varying Climate Sensitivity from Re-
438 gional Feedbacks. *Journal of Climate*, **26** (13), 4518–4534, URL [http://dx.doi.org/10.1175/](http://dx.doi.org/10.1175/JCLI-D-12-00544.1)
439 [JCLI-D-12-00544.1](http://dx.doi.org/10.1175/JCLI-D-12-00544.1).

440 Armour, K. C., J. Marshall, J. R. Scott, A. Donohoe, and E. R. Newsom, 2016: Southern ocean
441 warming delayed by circumpolar upwelling and equatorward transport. *Nature Geosci*, **9** (7),
442 549–554, URL <http://dx.doi.org/10.1038/ngeo2731>.

- 443 Bi, D., W. F. Budd, A. C. Hirst, and X. Wu, 2001: Collapse and reorganisation of the Southern
444 Ocean overturning under global warming in a coupled model. *Geophysical Research Letters*,
445 **28 (20)**, 3927–3930, URL <http://dx.doi.org/10.1029/2001GL013705>.
- 446 Bilbao, R. A., J. M. Gregory, and N. Bouttes, 2015: Analysis of the regional pattern of sea
447 level change due to ocean dynamics and density change for 1993–2099 in observations and
448 CMIP5 AOGCMs. *Climate Dynamics*, **45 (9-10)**, 2647–2666, URL <http://dx.doi.org/10.1007/s00382-015-2499-z>.
- 450 Bloch-Johnson, J., R. T. Pierrehumbert, and D. S. Abbot, 2015: Feedback temperature dependence
451 determines the risk of high warming. *Geophysical Research Letters*, **42 (12)**, 4973– 4980, doi:
452 10.1002/2015GL064240, URL <http://dx.doi.org/10.1002/2015GL064240>, 2015GL064240.
- 453 Bloch-Johnson, J., M. Rugenstein, and D. S. Abbot, in revision: Spatial radiative feedbacks from
454 interannual variability using multiple regression. *Journal of Climate*.
- 455 Block, K., and T. Mauritsen, 2013: Forcing and feedback in the MPI-ESM-LR coupled model
456 under abruptly quadrupled CO₂. *Journal of Advances in Modeling Earth Systems*, **5 (4)**, 676–
457 691, URL <http://dx.doi.org/10.1002/jame.20041>.
- 458 Boer, G., and B. Yu, 2003a: Climate sensitivity and climate state. *Climate Dynamics*, **21 (2)**,
459 167–176, URL <http://dx.doi.org/10.1007/s00382-003-0323-7>.
- 460 Boer, G., and B. Yu, 2003b: Climate sensitivity and response. *Climate Dynamics*, **20 (4)**, 415–429,
461 URL <http://dx.doi.org/10.1007/s00382-002-0283-3>.
- 462 Boer, G. J., and B. Yu, 2003c: Dynamical aspects of climate sensitivity. *Geophysical Research*
463 *Letters*, **30 (3)**, doi:10.1029/2002GL016549, URL <http://dx.doi.org/10.1029/2002GL016549>.

- 464 Brandefelt, J., and B. L. Otto-Bliesner, 2009: Equilibration and variability in a last
465 glacial maximum climate simulation with ccs3. *Geophysical Research Letters*, **36** (19),
466 doi:10.1029/2009GL040364, URL [https://agupubs.onlinelibrary.wiley.com/doi/abs/10.1029/
467 2009GL040364](https://agupubs.onlinelibrary.wiley.com/doi/abs/10.1029/2009GL040364).
- 468 Brown, P. T., Y. Ming, W. Li, and S. A. Hill, 2017: Change in the magnitude and mechanisms
469 of global temperature variability with warming. *Nature Climate Change*, **7**, 743 EP –, URL
470 <http://dx.doi.org/10.1038/nclimate3381>.
- 471 Burls, N. J., and A. V. Fedorov, 2017: Wetter subtropics in a warmer world: Contrasting past and
472 future hydrological cycles. *Proceedings of the National Academy of Sciences*, **114** (49), 12 888–
473 12 893, doi:10.1073/pnas.1703421114, URL <https://www.pnas.org/content/114/49/12888>.
- 474 Caballero, R., and M. Huber, 2013: State-dependent climate sensitivity in past warm climates and
475 its implications for future climate projections. *Proceedings of the National Academy of Sciences
476 of the United States of America*, **110** (35), 14 162–14 167, URL [http://www.ncbi.nlm.nih.gov/
477 pmc/articles/PMC3761583/](http://www.ncbi.nlm.nih.gov/pmc/articles/PMC3761583/).
- 478 Caldwell, P. M., M. D. Zelinka, K. E. Taylor, and K. Marvel, 2015: Quantifying the sources
479 of inter-model spread in equilibrium climate sensitivity. *Journal of Climate*, doi:10.1175/
480 JCLI-D-15-0352.1, URL <http://dx.doi.org/10.1175/JCLI-D-15-0352.1>.
- 481 Cao, L., L. Duan, G. Bala, and K. Caldeira, 2016: Simulated long-term climate response to
482 idealized solar geoengineering. *Geophysical Research Letters*, URL [http://dx.doi.org/10.1002/
483 2016GL068079](http://dx.doi.org/10.1002/2016GL068079).
- 484 Castruccio, S., D. J. McInerney, M. L. Stein, F. Liu Crouch, R. L. Jacob, and E. J. Moyer, 2014:
485 Statistical Emulation of Climate Model Projections Based on Precomputed GCM Runs. *Journal*

486 *of Climate*, **27** (5), 1829–1844, doi:10.1175/JCLI-D-13-00099.1, URL <https://doi.org/10.1175/JCLI-D-13-00099.1>,
487 <https://doi.org/10.1175/JCLI-D-13-00099.1>.

488 Ceppi, P., F. Brient, M. D. Zelinka, and D. L. Hartmann, 2017: Cloud feedback mechanisms and
489 their representation in global climate models. *Wiley Interdisciplinary Reviews: Climate Change*,
490 **8** (4), e465, doi:10.1002/wcc.465, URL <https://onlinelibrary.wiley.com/doi/abs/10.1002/wcc.465>,
491 <https://onlinelibrary.wiley.com/doi/pdf/10.1002/wcc.465>.

492 Ceppi, P., and J. M. Gregory, 2017: Relationship of tropospheric stability to climate sensitiv-
493 ity and earth’s observed radiation budget. *Proceedings of the National Academy of Sciences*,
494 **114** (50), 13 126–13 131, doi:10.1073/pnas.1714308114, URL [https://www.pnas.org/content/](https://www.pnas.org/content/114/50/13126)
495 [114/50/13126](https://www.pnas.org/content/114/50/13126).

496 Charney, J., and Coauthors, 1979: Carbon Dioxide and Climate: A Scientific Assessment. Tech.
497 rep., National Academy of Science, Washington, DC.

498 Clark, P. U., and Coauthors, 2016: Consequences of twenty-first-century policy for multi-
499 millennial climate and sea-level change. *Nature Climate Change*, **6**, 360 EP –, URL <http://dx.doi.org/10.1038/nclimate2923>.
500

501 Collins, W. J., and Coauthors, 2011: Development and evaluation of an Earth-System model
502 – HadGEM2. *Geoscientific Model Development*, **4** (4), 1051–1075, URL [https://www.
503 geosci-model-dev.net/4/1051/2011/](https://www.geosci-model-dev.net/4/1051/2011/).

504 Colman, R., and L. Hanson, 2016: On the relative strength of radiative feedbacks under climate
505 variability and change. *Climate Dynamics*, 1–15, doi:10.1007/s00382-016-3441-8, URL <http://dx.doi.org/10.1007/s00382-016-3441-8>.
506

507 Colman, R., and B. McAvaney, 2009: Climate feedbacks under a very broad range of forcing.
508 *Geophysical Research Letters*, **36** (1), n/a–n/a, doi:10.1029/2008GL036268, URL <http://dx.doi.org/10.1029/2008GL036268>.
509

510 Cox, P. M., R. A. Betts, C. D. Jones, S. A. Spall, and I. J. Totterdell, 2000: Acceleration of global
511 warming due to carbon-cycle feedbacks in a coupled climate model. *Nature*, **408**, 184 EP –,
512 URL <http://dx.doi.org/10.1038/35041539>.

513 Danabasoglu, G., and P. R. Gent, 2009: Equilibrium Climate Sensitivity: Is It Accurate to Use
514 a Slab Ocean Model? *Journal of Climate*, **22** (9), 2494–2499, URL <http://dx.doi.org/10.1175/2008JCLI2596.1>.
515

516 Danabasoglu, G., S. G. Yeager, Y.-O. Kwon, J. J. Tribbia, A. S. Phillips, and J. W. Hurrell, 2012:
517 Variability of the Atlantic Meridional Overturning Circulation in CCSM4. *Journal of Climate*,
518 URL <http://dx.doi.org/10.1175/JCLI-D-11-00463.1>.

519 Deser, C., A. Phillips, V. Bourdette, and H. Teng, 2012: Uncertainty in climate change pro-
520 jections: the role of internal variability. *Climate Dynamics*, **38** (3), 527–546, doi:10.1007/
521 s00382-010-0977-x, URL <https://doi.org/10.1007/s00382-010-0977-x>.

522 Donner, L. J., and Coauthors, 2011: The Dynamical Core, Physical Parameterizations, and
523 Basic Simulation Characteristics of the Atmospheric Component AM3 of the GFDL Global
524 Coupled Model CM3. *Journal of Climate*, **24** (13), 3484–3519, URL <https://doi.org/10.1175/2011JCLI3955.1>.
525

526 Dufresne, J.-L., and Coauthors, 2013: Climate change projections using the IPSL-CM5 Earth
527 System Model: from CMIP3 to CMIP5. *Climate Dynamics*, **40** (9), 2123–2165, URL <https://doi.org/10.1007/s00382-012-1636-1>.
528

- 529 Dunne, J. P., and Coauthors, 2012: GFDL's ESM2 global coupled climate-carbon Earth System
530 Models Part I: Physical formulation and baseline simulation characteristics. *Journal of Climate*.
- 531 Eby, M., and Coauthors, 2013: Historical and idealized climate model experiments: an inter-
532 comparison of Earth system models of intermediate complexity. *Climate of the Past*, **9 (3)**,
533 1111–1140, URL <http://www.clim-past.net/9/1111/2013/>.
- 534 Eyring, V., S. Bony, G. A. Meehl, C. A. Senior, B. Stevens, R. J. Stouffer, and K. E. Taylor,
535 2016: Overview of the Coupled Model Intercomparison Project Phase 6 (CMIP6) experimental
536 design and organization. *Geoscientific Model Development*, **9 (5)**, 1937–1958, doi:10.5194/
537 gmd-9-1937-2016, URL <https://www.geosci-model-dev.net/9/1937/2016/>.
- 538 Frölicher, T., and F. Joos, 2010: Reversible and irreversible impacts of greenhouse gas emissions in
539 multi-century projections with the NCAR global coupled carbon cycle-climate model. *Climate*
540 *Dynamics*, **35 (7-8)**, 1439–1459, doi:10.1007/s00382-009-0727-0, URL [http://dx.doi.org/10.](http://dx.doi.org/10.1007/s00382-009-0727-0)
541 [1007/s00382-009-0727-0](http://dx.doi.org/10.1007/s00382-009-0727-0).
- 542 Frölicher, T. L., and D. J. Paynter, 2015: Extending the relationship between global warming and
543 cumulative carbon emissions to multi-millennial timescales. *Environmental Research Letters*,
544 **10 (7)**, 075 002, URL <http://stacks.iop.org/1748-9326/10/i=7/a=075002>.
- 545 Frölicher, T. L., M. Winton, and J. L. Sarmiento, 2014: Continued global warming after
546 CO₂ emissions stoppage. *Nature Clim. Change*, **4 (1)**, 40–44, URL [http://dx.doi.org/10.1038/](http://dx.doi.org/10.1038/nclimate2060)
547 [nclimate2060](http://dx.doi.org/10.1038/nclimate2060).
- 548 Gebbie, G., and P. Huybers, 2019: The Little Ice Age and 20th-century deep Pacific cooling.
549 *Science*, **363 (6422)**, 70–74, doi:10.1126/science.aar8413, URL [http://science.sciencemag.org/](http://science.sciencemag.org/content/363/6422/70)
550 [content/363/6422/70](http://science.sciencemag.org/content/363/6422/70).

- 551 Gent, P. R., and Coauthors, 2011: The Community Climate System Model Version 4. *Journal of*
552 *Climate*, **24** (19), 4973–4991, URL <http://dx.doi.org/10.1175/2011JCLI4083.1>.
- 553 Geoffroy, O., and D. Saint-Martin, 2014: Pattern decomposition of the transient climate response.
554 *Tellus A: Dynamic Meteorology and Oceanography*, **66** (1), 23–393, doi:10.3402/tellusa.v66.
555 23393, URL <https://doi.org/10.3402/tellusa.v66.23393>.
- 556 Geoffroy, O., D. Saint-Martin, G. Bellon, A. Voldoire, D. Olivié, and S. Tytéca, 2013a: Transient
557 Climate Response in a Two-Layer Energy-Balance Model. Part II: Representation of the Ef-
558 ficacy of Deep-Ocean Heat Uptake and Validation for CMIP5 AOGCMs. *Journal of Climate*,
559 **26** (6), 1859–1876, URL <http://dx.doi.org/10.1175/JCLI-D-12-00196.1>.
- 560 Geoffroy, O., D. Saint-Martin, D. J. L. Olivié, A. Voldoire, G. Bellon, and S. Tytéca, 2013b:
561 Transient Climate Response in a Two-Layer Energy-Balance Model. Part I: Analytical Solution
562 and Parameter Calibration Using CMIP5 AOGCM Experiments. *Journal of Climate*, **26** (6),
563 1841–1857, URL <http://dx.doi.org/10.1175/JCLI-D-12-00195.1>.
- 564 Gillett, N. P., V. K. Arora, K. Zickfeld, S. J. Marshall, and W. J. Merryfield, 2011: Ongoing
565 climate change following a complete cessation of carbon dioxide emissions. *Nature Geosci*,
566 **4** (2), 83–87, URL <http://dx.doi.org/10.1038/ngeo1047>.
- 567 Good, P., T. Andrews, R. Chadwick, J.-L. Dufresne, J. M. Gregory, J. A. Lowe, N. Schaller,
568 and H. Shiogama, 2016: nonlinMIP contribution to CMIP6: model intercomparison project
569 for non-linear mechanisms: physical basis, experimental design and analysis principles (v1.0).
570 *Geoscientific Model Development*, **9** (11), 4019–4028, doi:10.5194/gmd-9-4019-2016, URL
571 <https://www.geosci-model-dev.net/9/4019/2016/>.

- 572 Good, P., J. Gregory, J. Lowe, and T. Andrews, 2013: Abrupt CO₂ experiments as tools for pre-
573 dicting and understanding CMIP5 representative concentration pathway projections. *Climate*
574 *Dynamics*, **40 (3-4)**, 1041–1053, URL <http://dx.doi.org/10.1007/s00382-012-1410-4>.
- 575 Good, P., and Coauthors, 2015: Nonlinear regional warming with increasing co2 concentrations.
576 *Nature Clim. Change*, **5 (2)**, 138–142, URL <http://dx.doi.org/10.1038/nclimate2498>.
- 577 Gottschalk, J., and Coauthors, 2019: Mechanisms of millennial-scale atmospheric co2 change
578 in numerical model simulations. *Quaternary Science Reviews*, **220**, 30 – 74, doi:<https://doi.org/10.1016/j.quascirev.2019.05.013>, URL <http://www.sciencedirect.com/science/article/pii/S0277379118310473>.
579
580
- 581 Gregory, J. M., 2000: Vertical heat transports in the ocean and their effect on time-dependent cli-
582 mate change. *Climate Dynamics*, **16**, 501–515, URL <http://dx.doi.org/10.1007/s003820000059>,
583 [10.1007/s003820000059](http://dx.doi.org/10.1007/s003820000059).
- 584 Gregory, J. M., T. Andrews, and P. Good, 2015: The inconstancy of the transient climate re-
585 sponse parameter under increasing CO₂. *Philosophical Transactions of the Royal Society of*
586 *London A: Mathematical, Physical and Engineering Sciences*, **373 (2054)**, URL <http://rsta.royalsocietypublishing.org/content/373/2054/20140417>.
587
- 588 Gregory, J. M., T. Andrews, P. Good, T. Mauritsen, and P. M. Forster, 2016: Small global-mean
589 cooling due to volcanic radiative forcing. *Climate Dynamics*, 1–13, URL <http://dx.doi.org/10.1007/s00382-016-3055-1>.
590
- 591 Gregory, J. M., and Coauthors, 2004: A new method for diagnosing radiative forcing and
592 climate sensitivity. *Geophysical Research Letters*, **31 (3)**, URL <http://dx.doi.org/10.1029/2003GL018747>.
593

- 594 Gregory, J. M., and Coauthors, 2005: A model intercomparison of changes in the Atlantic ther-
595 mohaline circulation in response to increasing atmospheric CO₂ concentration. *Geophys. Res.*
596 *Lett.*, **32** (L12703).
- 597 Hasumi, H., and S. Emori, 2004: K-1 Coupled GCM (MIROC) Description. Tech. rep., Center
598 for Climate System Research CCSR, University of Tokyo, National Institute for Environmental
599 Studies (NIES), Frontier Research Center for Global Change (FRCGC).
- 600 Hazeleger, W., and Coauthors, 2012: EC-Earth V2.2: description and validation of a new seamless
601 earth system prediction model. *Climate Dynamics*, **39** (11), 2611–2629, URL [https://doi.org/10.](https://doi.org/10.1007/s00382-011-1228-5)
602 [1007/s00382-011-1228-5](https://doi.org/10.1007/s00382-011-1228-5).
- 603 Held, I., M. Winton, K. Takahashi, T. L. Delworth, F. Zeng, and G. Vallis, 2010: Probing the
604 Fast and Slow Components of Global Warming by Returning Abruptly to Preindustrial Forcing.
605 *Journal of Climate*, **23**, 2418 – 2427.
- 606 Hobbs, W., M. D. Palmer, and D. Monselesan, 2016: An Energy Conservation Analysis of Ocean
607 Drift in the CMIP5 Global Coupled Models. *Journal of Climate*, **29** (5), 1639–1653, doi:10.
608 [1175/JCLI-D-15-0477.1](https://doi.org/10.1175/JCLI-D-15-0477.1), URL <http://dx.doi.org/10.1175/JCLI-D-15-0477.1>.
- 609 Jansen, M. F., L.-P. Nadeau, and T. M. Merlis, 2018: Transient versus Equilibrium Response
610 of the Ocean’s Overturning Circulation to Warming. *Journal of Climate*, **31** (13), 5147–5163,
611 doi:10.1175/JCLI-D-17-0797.1, URL <https://doi.org/10.1175/JCLI-D-17-0797.1>.
- 612 Jonko, A. K., K. M. Shell, B. M. Sanderson, and G. Danabasoglu, 2013: Climate Feedbacks
613 in CCSM3 under Changing CO₂ Forcing. Part II: Variation of Climate Feedbacks and Sen-
614 sitivity with Forcing. *Journal of Climate*, **26** (9), 2784–2795, URL [http://dx.doi.org/10.1175/](http://dx.doi.org/10.1175/JCLI-D-12-00479.1)
615 [JCLI-D-12-00479.1](http://dx.doi.org/10.1175/JCLI-D-12-00479.1).

- 616 Joshi, M., and J. Gregory, 2008: Dependence of the land-sea contrast in surface cli-
617 mate response on the nature of the forcing. *Geophysical Research Letters*, **35** (24),
618 doi:10.1029/2008GL036234, URL [https://agupubs.onlinelibrary.wiley.com/doi/abs/10.1029/
619 2008GL036234](https://agupubs.onlinelibrary.wiley.com/doi/abs/10.1029/2008GL036234).
- 620 Jungclaus, J. H., and Coauthors, 2006: Ocean Circulation and Tropical Variability in the Coupled
621 Model ECHAM5/MPI-OM. *Journal of Climate*, **19** (16), 3952–3972, URL [https://doi.org/10.
622 1175/JCLI3827.1](https://doi.org/10.1175/JCLI3827.1).
- 623 Khon, V. C., B. Schneider, M. Latif, W. Park, and C. Wengel, 2018: Evolution of Eastern Equa-
624 torial Pacific Seasonal and Interannual Variability in Response to Orbital Forcing During the
625 Holocene and Eemian From Model Simulations. *Geophysical Research Letters*, **45** (18), 9843–
626 9851, doi:10.1029/2018GL079337, URL [https://agupubs.onlinelibrary.wiley.com/doi/abs/10.
627 1029/2018GL079337](https://agupubs.onlinelibrary.wiley.com/doi/abs/10.1029/2018GL079337).
- 628 Klockmann, M., U. Mikolajewicz, and J. Marotzke, 2016: The effect of greenhouse gas concentra-
629 tions and ice sheets on the glacial AMOC in a coupled climate model. *Climate of the Past*, **12** (9),
630 1829–1846, doi:10.5194/cp-12-1829-2016, URL <https://www.clim-past.net/12/1829/2016/>.
- 631 Knutti, R., 2010: The end of model democracy? *Climatic Change*, **102**, 395–404.
- 632 Knutti, R., M. A. A. Rugenstein, and G. C. Hegerl, 2017: Beyond equilibrium climate sensitivity.
633 *Nature Geoscience*, **10**, 727 EP –, URL <http://dx.doi.org/10.1038/ngeo3017>.
- 634 Köhler, P., C. Nehrbass-Ahles, J. Schmitt, T. F. Stocker, and H. Fischer, 2017: A 156 kyr smoothed
635 history of the atmospheric greenhouse gases CO₂, CH₄, and N₂O and their radiative forcing.
636 *Earth System Science Data*, **9** (1), 363–387, doi:10.5194/essd-9-363-2017, URL [https://www.
637 earth-syst-sci-data.net/9/363/2017/](https://www.earth-syst-sci-data.net/9/363/2017/).

- 638 Kostov, Y., K. C. Armour, and J. Marshall, 2014: Impact of the atlantic meridional over-
639 turning circulation on ocean heat storage and transient climate change. *Geophysical Re-*
640 *search Letters*, **41 (6)**, 2108–2116, doi:10.1002/2013GL058998, URL [http://dx.doi.org/10.](http://dx.doi.org/10.1002/2013GL058998)
641 [1002/2013GL058998](http://dx.doi.org/10.1002/2013GL058998).
- 642 Krasting, J. P., R. J. Stouffer, S. M. Griffies, R. W. Hallberg, S. L. Malyshev, B. L. Samuels,
643 and L. T. Sentman, 2018: Role of Ocean Model Formulation in Climate Response Uncertainty.
644 *Journal of Climate*, **31 (22)**, 9313–9333, doi:10.1175/JCLI-D-18-0035.1, URL [https://doi.org/](https://doi.org/10.1175/JCLI-D-18-0035.1)
645 [10.1175/JCLI-D-18-0035.1](https://doi.org/10.1175/JCLI-D-18-0035.1), <https://doi.org/10.1175/JCLI-D-18-0035.1>.
- 646 Levermann, A., P. U. Clark, B. Marzeion, G. A. Milne, D. Pollard, V. Radic, and A. Robinson,
647 2013: The multimillennial sea-level commitment of global warming. *Proceedings of the Na-*
648 *tional Academy of Sciences*, **110 (34)**, 13 745–13 750, URL [http://www.pnas.org/content/110/](http://www.pnas.org/content/110/34/13745.abstract)
649 [34/13745.abstract](http://www.pnas.org/content/110/34/13745.abstract).
- 650 Li, C., J.-S. Storch, and J. Marotzke, 2013: Deep-ocean heat uptake and equilibrium cli-
651 mate response. *Climate Dynamics*, **40 (5-6)**, 1071–1086, URL [http://dx.doi.org/10.1007/](http://dx.doi.org/10.1007/s00382-012-1350-z)
652 [s00382-012-1350-z](http://dx.doi.org/10.1007/s00382-012-1350-z).
- 653 Luo, Y., J. Lu, F. Liu, and O. Garuba, 2017: The Role of Ocean Dynamical Thermostat in De-
654 laying the El Niño–Like Response over the Equatorial Pacific to Climate Warming. *Journal*
655 *of Climate*, **30 (8)**, 2811–2827, doi:10.1175/JCLI-D-16-0454.1, URL [https://doi.org/10.1175/](https://doi.org/10.1175/JCLI-D-16-0454.1)
656 [JCLI-D-16-0454.1](https://doi.org/10.1175/JCLI-D-16-0454.1).
- 657 Lutsko, N. J., and K. Takahashi, 2018: What Can the Internal Variability of CMIP5 Models Tell
658 Us about Their Climate Sensitivity? *Journal of Climate*, **31 (13)**, 5051–5069, doi:10.1175/
659 [JCLI-D-17-0736.1](https://doi.org/10.1175/JCLI-D-17-0736.1), URL <https://doi.org/10.1175/JCLI-D-17-0736.1>.

- 660 Maher, N., D. Matei, S. Milinski, and J. Marotzke, 2018: Enso change in climate projec-
661 tions: Forced response or internal variability? *Geophysical Research Letters*, **45** (20), 11,390–
662 11,398, doi:10.1029/2018GL079764, URL [https://agupubs.onlinelibrary.wiley.com/doi/abs/10.](https://agupubs.onlinelibrary.wiley.com/doi/abs/10.1029/2018GL079764)
663 1029/2018GL079764.
- 664 Maher, N., and Coauthors, 2019: The Max Planck Institute Grand Ensemble: Enabling the
665 Exploration of Climate System Variability. *Journal of Advances in Modeling Earth Systems*,
666 **0** (0), doi:10.1029/2019MS001639, URL [https://agupubs.onlinelibrary.wiley.com/doi/abs/10.](https://agupubs.onlinelibrary.wiley.com/doi/abs/10.1029/2019MS001639)
667 1029/2019MS001639.
- 668 Manabe, S., R. J. Stouffer, M. J. Spelman, and K. Bryan, 1991: Transient Responses of a Cou-
669 pled Ocean Atmosphere Model to Gradual Changes of Atmospheric CO₂. Part I. Annual Mean
670 Response. *Journal of Climate*, **4** (8), 785–818.
- 671 Marzocchi, A., and M. F. Jansen, 2017: Connecting antarctic sea ice to deep-ocean circula-
672 tion in modern and glacial climate simulations. *Geophysical Research Letters*, **44** (12), 6286–
673 6295, doi:10.1002/2017GL073936, URL [https://agupubs.onlinelibrary.wiley.com/doi/abs/10.](https://agupubs.onlinelibrary.wiley.com/doi/abs/10.1002/2017GL073936)
674 1002/2017GL073936.
- 675 Mauritsen, T., and R. Pincus, 2017: Committed warming inferred from observations. *Nature Cli-*
676 *mate Change*, **7**, 652 EP –, URL <https://doi.org/10.1038/nclimate3357>.
- 677 Mauritsen, T., and Coauthors, 2018: Developments in the mpi-m earth system model version 1.2
678 (mpi-esm 1.2) and its response to increasing co2. *Journal of Advances in Modeling Earth Sys-*
679 *tems*, **0** (ja), doi:10.1029/2018MS001400, URL [https://agupubs.onlinelibrary.wiley.com/doi/](https://agupubs.onlinelibrary.wiley.com/doi/abs/10.1029/2018MS001400)
680 [abs/10.1029/2018MS001400](https://agupubs.onlinelibrary.wiley.com/doi/abs/10.1029/2018MS001400).

681 Meehl, G. A., C. Covey, T. Delworth, M. Latif, B. McAvaney, J. F. B. Mitchell, R. J. Stouffer,
682 and K. E. Taylor, 2007: THE WCRP CMIP3 Multimodel Dataset: A New Era in Climate
683 Change Research. *Bulletin of the American Meteorological Society*, **88** (9), 1383–1394, doi:
684 10.1175/BAMS-88-9-1383, URL <https://doi.org/10.1175/BAMS-88-9-1383>.

685 Meraner, K., T. Mauritsen, and A. Voigt, 2013: Robust increase in equilibrium climate sensitivity
686 under global warming. *Geophysical Research Letters*, **40** (22), 5944–5948, URL <http://dx.doi.org/10.1002/2013GL058118>.

688 Miller, R. L., and Coauthors, 2014: CMIP5 historical simulations (1850–2012) with GISS Mod-
689 elE2. *Journal of Advances in Modeling Earth Systems*, **6** (2), 441–478, URL <http://dx.doi.org/10.1002/2013MS000266>.

691 Nazarenko, L., and Coauthors, 2015: Future climate change under RCP emission scenarios with
692 GISS ModelE2. *Journal of Advances in Modeling Earth Systems*, **7** (1), 244–267, URL <http://dx.doi.org/10.1002/2014MS000403>.

694 Paynter, D., T. L. Frölicher, L. W. Horowitz, and L. G. Silvers, 2018: Equilibrium Climate
695 Sensitivity Obtained From Multimillennial Runs of Two GFDL Climate Models. *Journal of*
696 *Geophysical Research: Atmospheres*, **123** (4), 1921–1941, doi:10.1002/2017JD027885, URL
697 <https://agupubs.onlinelibrary.wiley.com/doi/abs/10.1002/2017JD027885>.

698 Proistosescu, C., and P. J. Huybers, 2017: Slow climate mode reconciles historical and model-
699 based estimates of climate sensitivity. *Science Advances*, **3** (7), doi:10.1126/sciadv.1602821,
700 URL <http://advances.sciencemag.org/content/3/7/e1602821>.

701 Ramanathan, V., R. D. Cess, E. F. Harrison, P. Minnis, B. R. Barkstrom, E. Ahmad,
702 and D. Hartmann, 1989: Cloud-Radiative Forcing and Climate: Results from the Earth

- 703 Radiation Budget Experiment. *Science*, **243 (4887)**, 57–63, doi:10.1126/science.243.4887.
704 57, URL <https://science.sciencemag.org/content/243/4887/57>, [https://science.sciencemag.org/](https://science.sciencemag.org/content/243/4887/57.full.pdf)
705 [content/243/4887/57.full.pdf](https://science.sciencemag.org/content/243/4887/57.full.pdf).
- 706 Rehfeld, K., T. Münch, S. L. Ho, and T. Laepple, 2018: Global patterns of declining temperature
707 variability from the Last Glacial Maximum to the Holocene. *Nature*, **554**, 356 EP –, URL <https://doi.org/10.1038/nature25454>.
708
- 709 Rind, D., G. A. Schmidt, J. Jonas, R. Miller, L. Nazarenko, M. Kelley, and J. Romanski, 2018:
710 Multicentury Instability of the Atlantic Meridional Circulation in Rapid Warming Simula-
711 tions With GISS ModelE2. *Journal of Geophysical Research: Atmospheres*, **123 (12)**, 6331–
712 6355, doi:10.1029/2017JD027149, URL [https://agupubs.onlinelibrary.wiley.com/doi/abs/10.](https://agupubs.onlinelibrary.wiley.com/doi/abs/10.1029/2017JD027149)
713 [1029/2017JD027149](https://agupubs.onlinelibrary.wiley.com/doi/abs/10.1029/2017JD027149).
- 714 Rodgers, K. B., J. Lin, and T. L. Frölicher, 2015: Emergence of multiple ocean ecosystem drivers
715 in a large ensemble suite with an Earth system model. *Biogeosciences*, **12 (11)**, 3301–3320,
716 doi:10.5194/bg-12-3301-2015, URL <https://www.biogeosciences.net/12/3301/2015/>.
- 717 Rohrschneider, T., B. Stevens, and T. Mauritsen, 2019: On simple representations of the climate
718 response to external radiative forcing. *Climate Dynamics*, doi:10.1007/s00382-019-04686-4.
- 719 Rugenstein, M., and Coauthors, 2019: Equilibrium climate sensitivity estimated by equilibrating
720 climate models. *in revision for GRL*.
- 721 Rugenstein, M. A. A., K. Caldeira, and R. Knutti, 2016a: Dependence of global radiative feed-
722 backs on evolving patterns of surface heat fluxes. *Geophysical Research Letters*, **43 (18)**, 9877–
723 9885, URL <http://dx.doi.org/10.1002/2016GL070907>.

- 724 Rugenstein, M. A. A., J. M. Gregory, N. Schaller, J. Sedláček, and R. Knutti, 2016b: Multiannual
725 Ocean–Atmosphere Adjustments to Radiative Forcing. *Journal of Climate*, **29** (15), 5643–5659,
726 URL <http://dx.doi.org/10.1175/JCLI-D-16-0312.1>.
- 727 Rugenstein, M. A. A., J. Sedláček, and R. Knutti, 2016c: Nonlinearities in patterns of long-term
728 ocean warming. *Geophysical Research Letters*, **43** (7), 3380–3388, URL [http://dx.doi.org/10.](http://dx.doi.org/10.1002/2016GL068041)
729 [1002/2016GL068041](http://dx.doi.org/10.1002/2016GL068041).
- 730 Saint-Martin, D., and Coauthors, 2019: Fast forward to perturbed equilibrium climate.
731 *Geophysical Research Letters*, **0** (ja), doi:10.1029/2019GL083031, URL [https://agupubs.](https://agupubs.onlinelibrary.wiley.com/doi/abs/10.1029/2019GL083031)
732 [onlinelibrary.wiley.com/doi/abs/10.1029/2019GL083031](https://agupubs.onlinelibrary.wiley.com/doi/abs/10.1029/2019GL083031), [https://agupubs.onlinelibrary.wiley.](https://agupubs.onlinelibrary.wiley.com/doi/pdf/10.1029/2019GL083031)
733 [com/doi/pdf/10.1029/2019GL083031](https://agupubs.onlinelibrary.wiley.com/doi/pdf/10.1029/2019GL083031).
- 734 Salzmann, M., 2017: The polar amplification asymmetry: role of Antarctic surface height.
735 *Earth System Dynamics*, **8** (2), 323–336, doi:10.5194/esd-8-323-2017, URL [https://www.](https://www.earth-syst-dynam.net/8/323/2017/)
736 [earth-syst-dynam.net/8/323/2017/](https://www.earth-syst-dynam.net/8/323/2017/).
- 737 Scheff, J., R. Seager, H. Liu, and S. Coats, 2017: Are Glacials Dry? Consequences for Pa-
738 leoclimatology and for Greenhouse Warming. *Journal of Climate*, **30** (17), 6593–6609, doi:
739 [10.1175/JCLI-D-16-0854.1](https://doi.org/10.1175/JCLI-D-16-0854.1), URL <https://doi.org/10.1175/JCLI-D-16-0854.1>.
- 740 Schmidt, G. A., and Coauthors, 2014: Configuration and assessment of the GISS ModelE2 contri-
741 butions to the CMIP5 archive. *Journal of Advances in Modeling Earth Systems*, **6** (1), 141–184,
742 URL <http://dx.doi.org/10.1002/2013MS000265>.
- 743 Schneider, T., C. M. Kaul, and K. G. Pressel, 2019: Possible climate transitions from breakup
744 of stratocumulus decks under greenhouse warming. *Nature Geoscience*, **12** (3), 163–167, doi:
745 [10.1038/s41561-019-0310-1](https://doi.org/10.1038/s41561-019-0310-1), URL <https://doi.org/10.1038/s41561-019-0310-1>.

- 746 Senior, C. A., and J. F. B. Mitchell, 2000: The time-dependence of climate sensitivity. *Geophysical*
747 *Research Letters*, **27** (17), 2685–2688, URL <http://dx.doi.org/10.1029/2000GL011373>.
- 748 Smith, R. S., J. M. Gregory, and A. Osprey, 2008: A description of the FAMOUS (version XD-
749 BUA) climate model and control run. *Geoscientific Model Development*, **1** (1), 53–68, doi:
750 10.5194/gmd-1-53-2008, URL <https://www.geosci-model-dev.net/1/53/2008/>.
- 751 Sniderman, J. M. K., and Coauthors, 2019: Southern Hemisphere subtropical drying as a transient
752 response to warming. *Nature Climate Change*, doi:10.1038/s41558-019-0397-9, URL <https://doi.org/10.1038/s41558-019-0397-9>.
- 754 Song, X., and G. J. Zhang, 2014: Role of Climate Feedback in El Niño-like SST Response to
755 Global Warming. *Journal of Climate*, doi:10.1175/JCLI-D-14-00072.1, URL [http://dx.doi.org/](http://dx.doi.org/10.1175/JCLI-D-14-00072.1)
756 [10.1175/JCLI-D-14-00072.1](http://dx.doi.org/10.1175/JCLI-D-14-00072.1).
- 757 Stouffer, R., and S. Manabe, 2003: Equilibrium response of thermohaline circulation to large
758 changes in atmospheric CO₂ concentration. *Climate Dynamics*, **20** (7-8), 759–773, URL <http://dx.doi.org/10.1007/s00382-002-0302-4>.
- 760 Stouffer, R. J., and S. Manabe, 1999: Response of a Coupled Ocean–Atmosphere Model to
761 Increasing Atmospheric Carbon Dioxide: Sensitivity to the Rate of Increase. *Journal of Cli-*
762 *mate*, **12** (8), 2224–2237, doi:10.1175/1520-0442(1999)012<2224:ROACOA>2.0.CO;2, URL
763 [http://dx.doi.org/10.1175/1520-0442\(1999\)012<2224:ROACOA>2.0.CO;2](http://dx.doi.org/10.1175/1520-0442(1999)012<2224:ROACOA>2.0.CO;2).
- 764 Svendsen, S. H., M. S. Madsen, Y. Suting, C. Rodehacke, and G. Adalgeirsdottir, 2015: An Intro-
765 duction to the Coupled EC-Earth-PISM Model System. report 15-05, Danish Climate Centre.

- 766 Taylor, K. E., R. J. Stouffer, and G. A. Meehl, 2011: An Overview of CMIP5 and the Ex-
767 periment Design. *Bulletin of the American Meteorological Society*, **93** (4), 485–498, doi:
768 10.1175/BAMS-D-11-00094.1, URL <http://dx.doi.org/10.1175/BAMS-D-11-00094.1>.
- 769 Thomas, M. D., and A. V. Fedorov, 2019: Mechanisms and Impacts of a Partial AMOC
770 Recovery Under Enhanced Freshwater Forcing. *Geophysical Research Letters*, **0** (0),
771 doi:10.1029/2018GL080442, URL [https://agupubs.onlinelibrary.wiley.com/doi/abs/10.1029/](https://agupubs.onlinelibrary.wiley.com/doi/abs/10.1029/2018GL080442)
772 2018GL080442.
- 773 Trossman, D. S., J. B. Palter, T. M. Merlis, Y. Huang, and Y. Xia, 2016: Large-scale ocean
774 circulation-cloud interactions reduce the pace of transient climate change. *Geophysical Re-*
775 *search Letters*, **43** (8), 3935–3943, URL <http://dx.doi.org/10.1002/2016GL067931>.
- 776 Vial, J., J.-L. Dufresne, and S. Bony, 2013: On the interpretation of inter-model spread in CMIP5
777 climate sensitivity estimates. *Climate Dynamics*, **41** (11-12), 3339–3362, URL [http://dx.doi.org/](http://dx.doi.org/10.1007/s00382-013-1725-9)
778 10.1007/s00382-013-1725-9.
- 779 Voldoire, A., and Coauthors, 2019: Evaluation of cmip6 deck experiments with cnrm-cm6-
780 1. *Journal of Advances in Modeling Earth Systems*, **0** (0), doi:10.1029/2019MS001683,
781 URL <https://agupubs.onlinelibrary.wiley.com/doi/abs/10.1029/2019MS001683>, <https://agupubs.onlinelibrary.wiley.com/doi/pdf/10.1029/2019MS001683>.
- 783 Voss, R., and U. Mikolajewicz, 2001: Long-term climate changes due to increased CO2 con-
784 centration in the coupled atmosphere-ocean general circulation model ECHAM3/LSG. *Climate*
785 *Dynamics*, **17** (1), 45–60, doi:10.1007/PL00007925, URL <https://doi.org/10.1007/PL00007925>.
- 786 Winton, M., K. Takahashi, and I. M. Held, 2010: Importance of Ocean Heat Uptake Efficacy to
787 Transient Climate Change. *Journal of Climate*, **23** (9), 2333–2344, doi:10.1175/2009JCLI3139.

788 1, URL <http://dx.doi.org/10.1175/2009JCLI3139.1>.

789 Yamamoto, A., A. Abe-Ouchi, M. Shigemitsu, A. Oka, K. Takahashi, R. Ohgaito, and Y. Ya-
790 manaka, 2015: Global deep ocean oxygenation by enhanced ventilation in the Southern Ocean
791 under long-term global warming. *Global Biogeochemical Cycles*, **29** (10), 1801–1815, URL
792 <http://dx.doi.org/10.1002/2015GB005181>.

793 Yeager, S. G., C. A. Shields, W. G. Large, and J. J. Hack, 2006: The Low-Resolution CCSM3.
794 *Journal of Climate*, **19** (11), 2545–2566, URL <http://dx.doi.org/10.1175/JCLI3744.1>.

795 Yoshimori, M., M. Watanabe, H. Shiogama, A. Oka, A. Abe-Ouchi, R. Ohgaito, and Y. Kamae,
796 2016: A review of progress towards understanding the transient global mean surface temper-
797 ature response to radiative perturbation. *Progress in Earth and Planetary Science*, **3** (1), 21,
798 doi:10.1186/s40645-016-0096-3, URL <https://doi.org/10.1186/s40645-016-0096-3>.

799 Zhang, X., G. Lohmann, G. Knorr, and X. Xu, 2013: Different ocean states and transient character-
800 istics in last glacial maximum simulations and implications for deglaciation. *Climate of the Past*,
801 **9** (5), 2319–2333, doi:10.5194/cp-9-2319-2013, URL <https://www.clim-past.net/9/2319/2013/>.

802 Zhou, C., M. D. Zelinka, and S. A. Klein, 2016: Impact of decadal cloud variations on the Earth’s
803 energy budget. *Nature Geosci*, **9** (12), 871–874, URL <http://dx.doi.org/10.1038/ngeo2828>.

804 Zhu, J., Z. Liu, J. Zhang, and W. Liu, 2014: AMOC response to global warming: dependence on
805 the background climate and response timescale. *Climate Dynamics*, **44** (11), 3449–3468, URL
806 <http://dx.doi.org/10.1007/s00382-014-2165-x>.

807 Zickfeld, K., and Coauthors, 2013: Long-Term Climate Change Commitment and Reversibility:
808 An EMIC Intercomparison. *Journal of Climate*, **26** (16), 5782–5809, URL <http://dx.doi.org/10.1175/JCLI-D-12-00584.1>.

809

810 **LIST OF TABLES**

811 **Table 1.** Description of collected variables. 2D means spatial resolution of latitude and
812 longitude, except for *msfmyz* where it means latitude and depth. 3D means lat-
813 itude, longitude, and depth. *msfmyz* is the sum of the eularian, eddybolus, and
814 submeso component. For *so* and *thetao* there are also February and September
815 values available for most models. 39

816 **Table 2.** Overview of models and contributed simulations. The resolution of atmosphere
817 and ocean is given in # of grid points per latitude x longitude, and latitude x
818 longitude x depth, respectively. Models are referred to by their shortnames
819 throughout the manuscript. Section 2b describes the forcing levels. References
820 in the last column describe the models and simulations. Some simulations are
821 published in their full length, some simulations contributed to LongRunMIP are
822 the extensions of simulations discussed in the references, and some simulations
823 are unpublished. 40

824 **Table 3.** Published millennial-length simulations 41

825 TABLE 1. Description of collected variables. 2D means spatial resolution of latitude and longitude, except for
826 *msftmyz* where it means latitude and depth. 3D means latitude, longitude, and depth. *msftmyz* is the sum of the
827 eularian, eddybolus, and submeso component. For *so* and *thetao* there are also February and September values
828 available for most models.

Shortname	Longname	Unit	Resolution
hfls	Surface Upward Latent Heat Flux	W m^{-2}	monthly, 2D
hfss	Surface Upward Sensible Heat Flux	W m^{-2}	monthly, 2D
pr	Precipitation on atmospheric grid	$\text{kg m}^{-2} \text{s}^{-1}$	monthly, 2D
psl	Sea Level Pressure	Pa	monthly, 2D
rlds	Surface Downwelling Longwave Radiation	W m^{-2}	monthly, 2D
rlus	Surface Upwelling Longwave Radiation	W m^{-2}	monthly, 2D
rlut	TOA Outgoing Longwave Radiation	W m^{-2}	monthly, 2D
rlutcs	TOA Outgoing Clear-Sky Longwave Radiation	W m^{-2}	monthly, 2D
rsds	Surface Downwelling Shortwave Radiation	W m^{-2}	monthly, 2D
rsdt	TOA Incident Shortwave Radiation	W m^{-2}	monthly, 2D
rsus	Surface Upwelling Shortwave Radiation	W m^{-2}	monthly, 2D
rsut	TOA Outgoing Shortwave Radiation	W m^{-2}	monthly, 2D
rsutcs	TOA Outgoing Clear-Sky Shortwave Radiation	W m^{-2}	monthly, 2D
tas	Near-Surface Air Temperature	K	monthly, 2D
ts	Atmospheric surface temperature	K	monthly, 2D
sic	Sea Ice Area Fraction	%	monthly, 2D
msftmyz	Meridional Overturning Circulation	$\text{m}^3 \text{s}^{-1}$	annual, 2D
tos	Sea surface temperature	K	annual, 2D
sos	Sea surface salinity	psu	annual, 2D
wfo	Net water flux into sea water	$\text{kg m}^{-2} \text{s}^{-1}$	annual, 2D
evs	Water evaporation	$\text{kg m}^{-2} \text{s}^{-1}$	annual, 2D
pr_ocn	Precipitation (rain and snow) on ocean grid	$\text{kg m}^{-2} \text{s}^{-1}$	annual, 2D
tauuo	Surface downward wind stress in x direction	N m^{-2}	annual, 2D
tauvo	Surface downward wind stress in y direction	N m^{-2}	annual, 2D
so	Sea Water Salinity	psu	annual, 3D
thetao	Sea Water Potential Temperature	K	annual, 3D

829 TABLE 2. Overview of models and contributed simulations. The resolution of atmosphere and ocean is given
830 in # of grid points per latitude x longitude, and latitude x longitude x depth, respectively. Models are referred
831 to by their shortnames throughout the manuscript. Section 2b describes the forcing levels. References in the
832 last column describe the models and simulations. Some simulations are published in their full length, some
833 simulations contributed to LongRunMIP are the extensions of simulations discussed in the references, and some
834 simulations are unpublished.

Model (shortname)	Forcing level shortname	Length (yrs)	Atmosphere resolution	Ocean resolution	Control sim (yrs)	Model and simulation documentation
CCSM3 CCSM3	abrupt2x abrupt4x abrupt8x	3000 2120 1450	48 x 96	100 x 116 x 25	1530	Yeager et al. (2006) Danabasoglu and Gent (2009)
CCSM3 CCSM3II	abrupt2.4 abrupt4.8 lin2.4	3701 3132 3990	48 x 96	100 x 116 x 25	3805	Yeager et al. (2006) Castruccio et al. (2014)
CESM 1.0.4 CESM104	abrupt2x abrupt4x abrupt8x	2500 5900 5100	96 x 144	384 x 20 x 60	1320	Gent et al. (2011) Danabasoglu et al. (2012) Rugenstein et al. (2016c)
CNRM-CM6-1 CNRMCM61	abrupt2x abrupt4x	750 1850	128 x 256	180 x 360 x 75	2000	Voldoire et al. (2019) Saint-Martin et al. (2019)
EC-Earth-PISM ECEARTH	historical RCP8.5+	1270	160 x 320	292 x 362 x 42	508	Hazeleger et al. (2012) Svendsen et al. (2015)
ECHAM5/MPIOM ECHAM5	abrupt4x 1pct4x	1000 6080	48 x 96	101 x 120 x 40	100	Jungclauss et al. (2006) Li et al. (2013)
FAMOUS FAMOUS	abrupt2x abrupt4x	3000 3000	37 x 48	73 x 96 x 20	3000	Smith et al. (2008)
GFDL-CM3 GFDLCM3	1pct2x	5000	90 x 144	200 x 360 x 50	5200	Donner et al. (2011) Paynter et al. (2018)
GFDL-ESM2M GFDLESM2M	1pct2x	4500	90 x 144	200 x 360 x 50	1340	Dunne et al. (2012) Paynter et al. (2018)
GISS-E2-R GISSE2R	abrupt4x 1pct4x	5000 5000	90 x 144	180 x 288 x 32	5225	Schmidt et al. (2014); Miller et al. (2014); Nazarenko et al. (2015) Rind et al. (2018)
HadCM3L HadCM3L	abrupt2x abrupt4x abrupt6x abrupt8x	1000 1000 1000 1000	73 x 96	73 x 96 x 20	1000	Cox et al. (2000) Cao et al. (2016)
HadGEM2-ES HadGEM2	abrupt4x	1328	145 x 192	216 x 360 x 40	239	Collins et al. (2011) Andrews et al. (2015)
IPSL-CM5A-LR IPSLCM5ALR	abrupt4x	1000	96 x 96	149 x 182 x 31	1000	Dufresne et al. (2013)
MIROC 3.2 MIROC32	1pct2x 1pct4x	2000 2000	64 x 128	192 x 256 x 44	681	Hasumi and Emori (2004) Yamamoto et al. (2015); Yoshimori et al. (2016)
MPIESM-1.2 MPIESM12	abrupt2x abrupt4x abrupt8x abrupt16x	1000 1000 1000 1000	96 x 192	220 x 256 x 40	1237	Mauritsen et al. (2018) Rohrschneider et al. (2019)
MPIESM-1.1 MPIESM11	abrupt4x	4459	96 x 192	220 x 256 x 40	2000	Mauritsen et al. (2018)

TABLE 3. Published millennial-length simulations

Paper	Model	Forcing level	Length (yr)	Content/scientific comment
Senior and Mitchell (2000)	HadCM2	2xCO ₂	≈ 800	Included flux adjustments; effective climate sensitivity increases due to SW CRE due to changes in the inter-hemispheric temperature gradient
Bi et al. (2001)	CSIRO	3xCO ₂	≈ 1000	Cessation and recovery of Antarctic Bottom Water and North Atlantic Deep Water formation
Voss and Mikolajewicz (2001)	ECHAM3	2x, 4xCO ₂	850	Adjustment time scales, committed warming, ocean thermohaline circulation
Stouffer and Manabe (1999, GFDL 2003)	GFDL	0.5x, 2x, 4xCO ₂	4000	Thermohaline circulation and paleo-oceanographic implications
Boer and Yu (2003b,a,c)	CCCma	21st century	1000	Radiative feedbacks and surface warming; effective climate sensitivity decreases with time; slab versus fully coupled models
Gregory et al. (2004)	HadCM3	2xCO ₂	≈ 1000	TOA radiative imbalance and surface temperature are not linearly related; after 1000 yr the model is still 0.7 W m ⁻² away from equilibrium
* Danabasoglu and Gent (2009)	CCSM3	2x, 4x, 8xCO ₂	3000	Comparing slab and fully coupled models; determining ECS; Jonko et al. (2013) analyzed the contributions of different feedbacks to doublings of CO ₂
Gillett et al. (2011)	CanESM1	21st century	≈ 1000	Impact of reduced emissions
* Li et al. (2013)	ECHAM5/MPI-OM	2xCO ₂	≈ 6000	Comparing slab and fully coupled models; determining ECS; adjustment time scales of surface warming patterns, ocean heat uptake, and sea level rise
Frölicher et al. (2014); Frölicher and Paynter (2015)	GFDL-ESM2M, CSM1	4xCO ₂ pulse	1000	Climate impact of CO ₂ emission stoppage; evolving feedbacks; ECS; transient climate response to cumulative carbon emissions
* Andrews et al. (2015)	HadGEM2-ES	4xCO ₂	≈ 1300	Non-constancy of feedbacks; variations of TOA components cancel each other on the century to millennial time scale
* Yamamoto et al. (2015); MIROC 3.2 Yoshimori et al. (2016)	MIROC 3.2	2x, 4xCO ₂	2000	Deep ocean ventilation overall increases oxygenation after a transient decrease; review article on ocean heat uptake in coupled models and energy balance models
* Cao et al. (2016)	HadCM3L	2x, 4x, 6x, 8xCO ₂	1000	Comparing CO ₂ to other forcing agents and geo-engineering scenarios
* Rugenstein et al. (2016b,a)	CESM104	2x, 4x, 8xCO ₂	≈ 1300	Dependence of global and regional radiative feedback evolution on surface heat flux patterns; forcing adjustment
* Paynter et al. (2018)	GFDL-ESM2M, CM3	GFDL- 2xCO ₂	≈ 5000	Evolution of global and regional radiative feedbacks and the role of atmospheric vertical velocity fields and inversion strengths
* Rind et al. (2018)	GISS-E2-R	4xCO ₂	≈ 2000	AMOC reduction and recovery on North Atlantic surface flux conditions
Krasting et al. (2018)	GFDL-ESM2Mb, GFDL-ESM2G	4xCO ₂	5000	Ocean heat uptake, model formulation of diapycnal diffusivity and ocean vertical coordinates

835 **LIST OF FIGURES**

836 **Fig. 1.** Global and annual mean surface air temperature (*tas* in Table 1) anomaly and top of the
837 atmosphere (TOA) radiative imbalance (computed as $rsdt - rlut - rsut$, see Table 1) to a step-
838 forcing of quadrupling CO₂ as simulated by the CESM104 model. For the Coupled Model
839 Intercomparison Project Phase 5 and 6, this simulation is part of the standard protocol, but
840 only 150 simulated years are requested (blue shading). We collect simulations that extended
841 this experiment for at least 850 years (light red shading), ideally until they are equilibrated
842 (end of dark red shading). 43

843 **Fig. 2.** Global annual mean surface air temperature for all control (black) and forced (color, listed
844 in the top right of each panel) simulations. *abrupt2x, 4x, 6x, 8x* means that the CO₂ concen-
845 tration is doubled, quadrupled, sextupled, octupliated, as a step-forcing branched off the
846 control simulation. *1pct2x* and *1pct4x* means the CO₂ concentration is linearly increased
847 1 % per year until the concentration is doubled or quadrupled, respectively. The simula-
848 tions of ECEARTH and CCSM3II are described in Section b. Note the different axis ranges
849 for each model. GFDLCM3 and CCSM3II are not branched off directly from the control
850 simulation. 44

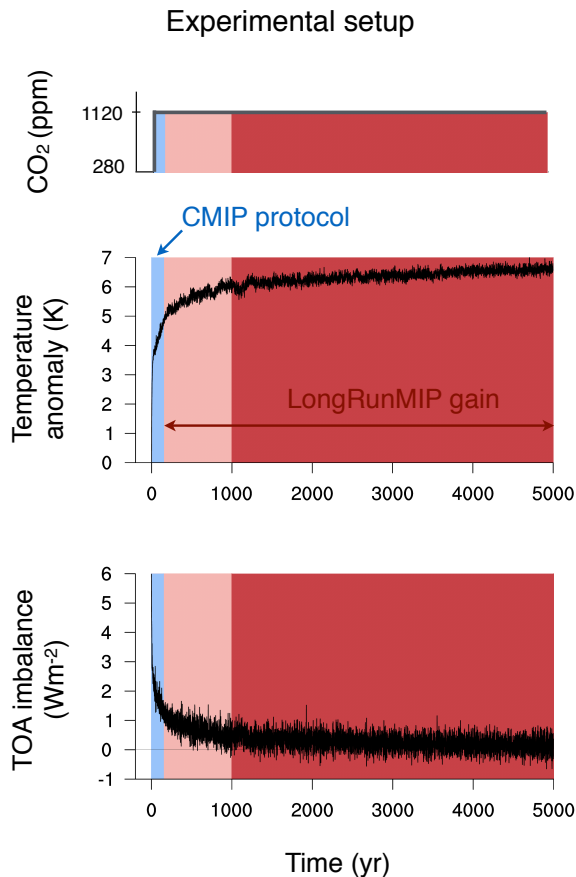
851 **Fig. 3.** Top of the atmosphere (TOA) annual and global mean radiative imbalance of all control
852 simulations. Note the different lengths of the horizontal axes. The gray line indicates the
853 average, the red line the linear trend, except for CCSM3II and GFDLCM3 for which both
854 colors depict a fourth-order-polynomial fit. 45

855 **Fig. 4.** Global and annual mean temperature anomalies (experiment minus average of the control
856 simulation) of the surface ocean (a, first layer) and deep ocean (b), as well as absolute values
857 of deep ocean temperature in the control simulations (c), for *abrup4x* (solid) and *1pct4x*
858 (dashed) simulations. “Deep ocean” means around 2000 m depth (closest level). Note that
859 the time scale in c) is shorter than in a) and b). 46

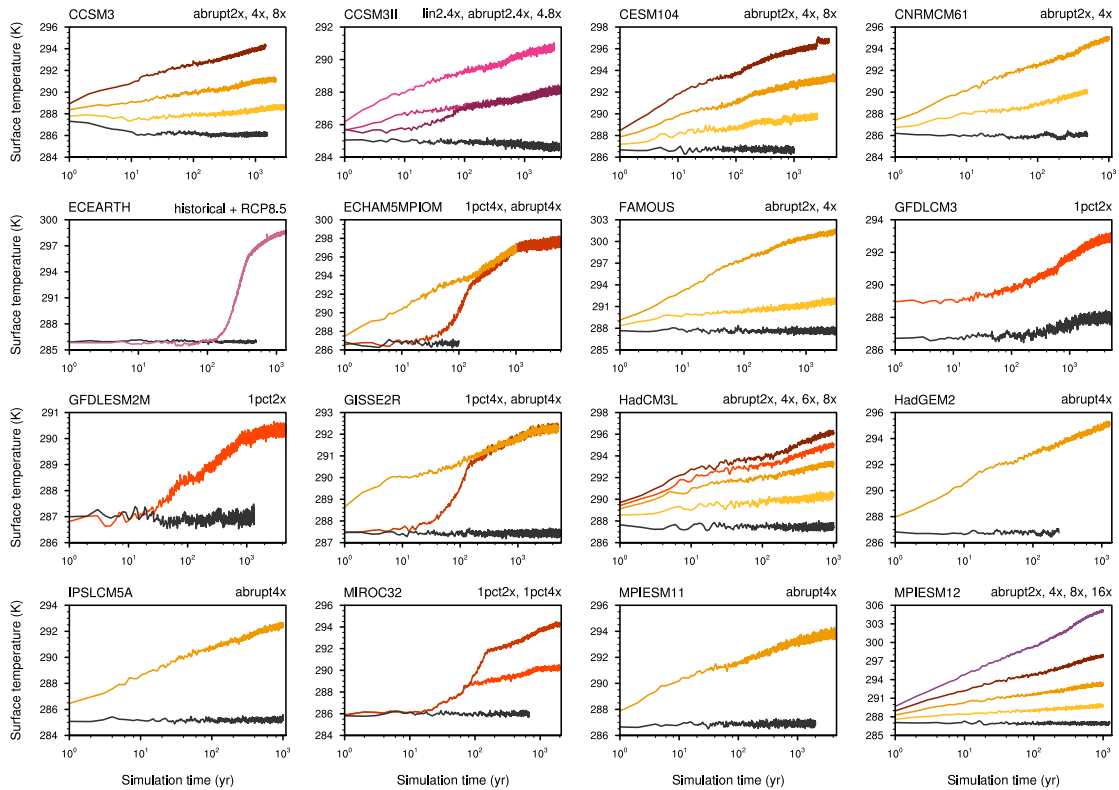
860 **Fig. 5.** Time evolution of the surface air temperature anomaly in the *abrupt4x* simulations. The
861 model mean of CCSM3, CESM104, CNRMCM61, ECHAM5, GISS2R, HadCM3L,
862 HadGEM2, IPSLCM5A, MPIESM11, and MPIESM12 is shown in panel a, b, c, e, and
863 f, while the model mean of only CESM104, GISS2R, and MPIESM11 is shown in panel d
864 and g, due to the length of these contributions. See Table 2 for details of the length of each
865 simulation. 47

866 **Fig. 6.** Time evolution of the zonal mean surface air temperature response normalized by the global
867 mean temperature anomaly. Above (below) 1 means that warming is amplified (reduced)
868 relative to the globally mean warming (a-d). Panel e-g show the differences (note the differ-
869 ence scale). Panel a, b, e, and f contain only *abrupt4x* simulations, while panel c, d, and g
870 also contain the *1pct2x* and *RCP8.5+* simulations with integration lengths above 4000 years.
871 Table 2 lists all simulations and model long names. 48

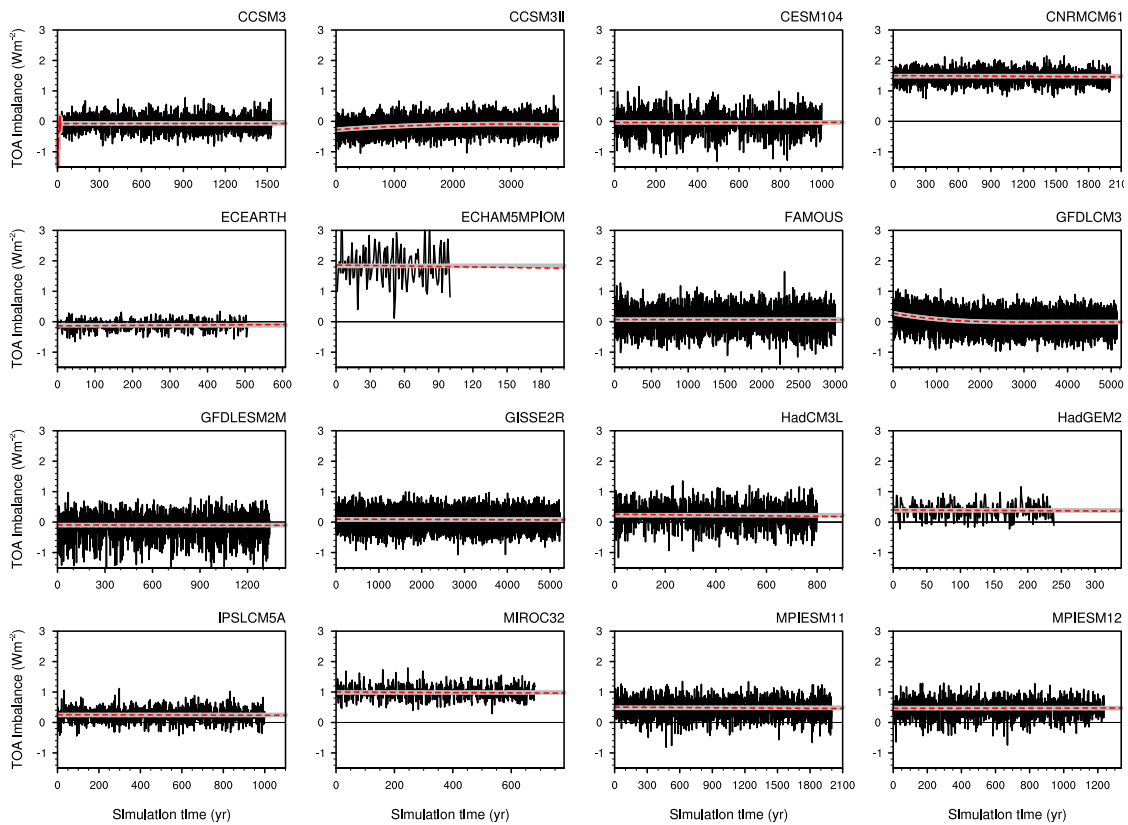
872 **Fig. 7.** Simulated shortwave cloud radiative effects SW CRE for different levels of global surface
873 air temperature changes. Each point is a ten-year running average. Note the different axes
874 labels, which cover a large range in TOA imbalance and surface temperature. Table 2 lists
875 all simulations and model long names. 49



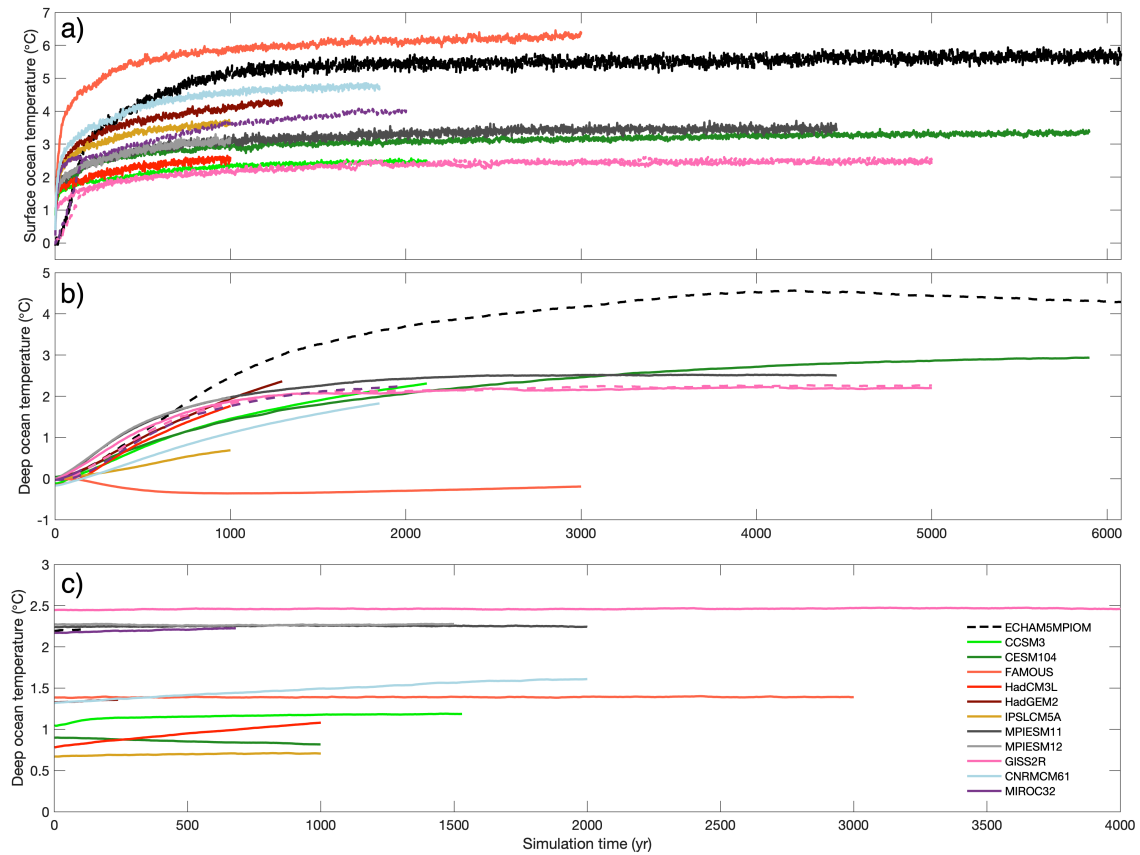
876 FIG. 1. Global and annual mean surface air temperature (*tas* in Table 1) anomaly and top of the atmosphere
 877 (TOA) radiative imbalance (computed as $rsdt - rlut - rsut$, see Table 1) to a step-forcing of quadrupling CO₂
 878 as simulated by the CESM104 model. For the Coupled Model Intercomparison Project Phase 5 and 6, this
 879 simulation is part of the standard protocol, but only 150 simulated years are requested (blue shading). We
 880 collect simulations that extended this experiment for at least 850 years (light red shading), ideally until they are
 881 equilibrated (end of dark red shading).



882 FIG. 2. Global annual mean surface air temperature for all control (black) and forced (color, listed in the top
 883 right of each panel) simulations. *abrupt2x, 4x, 6x, 8x* means that the CO₂ concentration is doubled, quadrupled,
 884 sextupled, octupliated, as a step-forcing branched off the control simulation. *1pct2x* and *1pct4x* means the CO₂
 885 concentration is linearly increased 1 % per year until the concentration is doubled or quadrupled, respectively.
 886 The simulations of ECEARTH and CCSM3II are described in Section b. Note the different axis ranges for each
 887 model. GFDLCM3 and CCSM3II are not branched off directly from the control simulation.

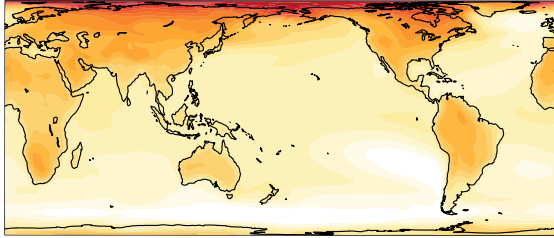


888 FIG. 3. Top of the atmosphere (TOA) annual and global mean radiative imbalance of all control simulations.
 889 Note the different lengths of the horizontal axes. The gray line indicates the average, the red line the linear trend,
 890 except for CCSM3II and GFDLCM3 for which both colors depict a fourth-order-polynomial fit.

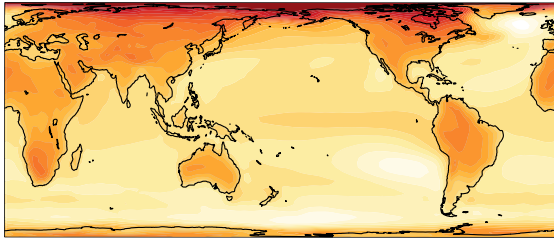


891 FIG. 4. Global and annual mean temperature anomalies (experiment minus average of the control simulation)
 892 of the surface ocean (a, first layer) and deep ocean (b), as well as absolute values of deep ocean temperature in
 893 the control simulations (c), for *abrup4x* (solid) and *1pct4x* (dashed) simulations. “Deep ocean” means around
 894 2000 m depth (closest level). Note that the time scale in c) is shorter than in a) and b).

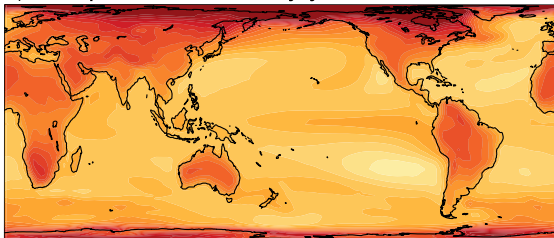
a) Temperature anomaly year 15-25



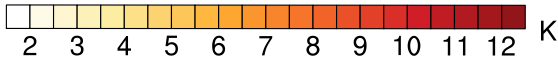
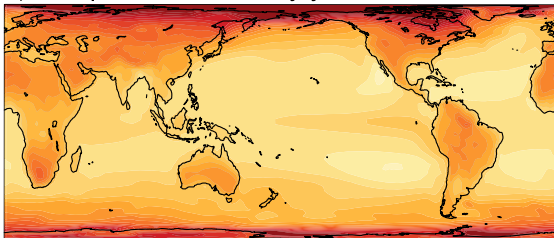
b) Temperature anomaly year 80-120



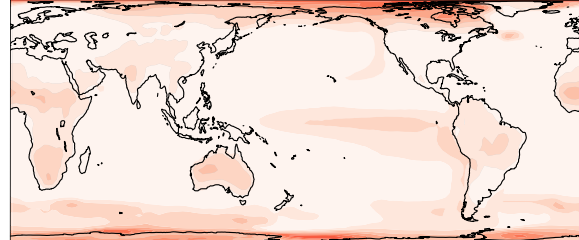
c) Temperature anomaly year 900-1000



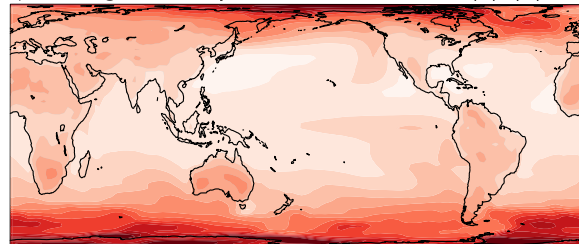
d) Temperature anomaly year 4000-4200



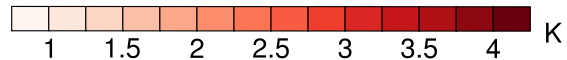
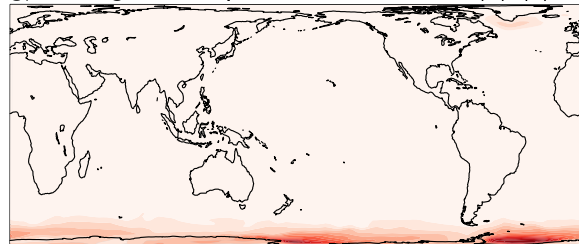
e) Change in temperature anomalies (b)-(a)



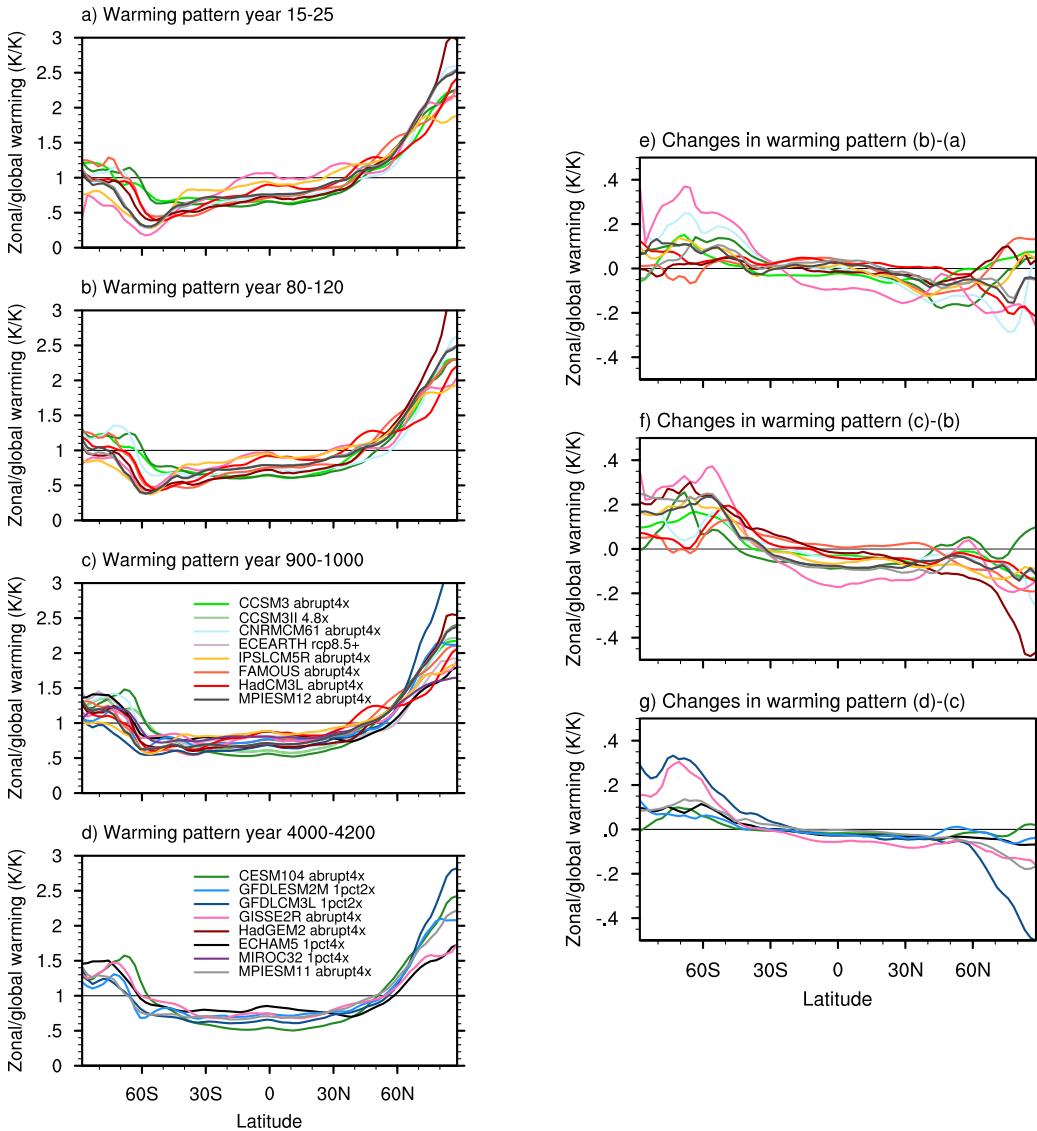
f) Change in temperature anomalies (c)-(b)



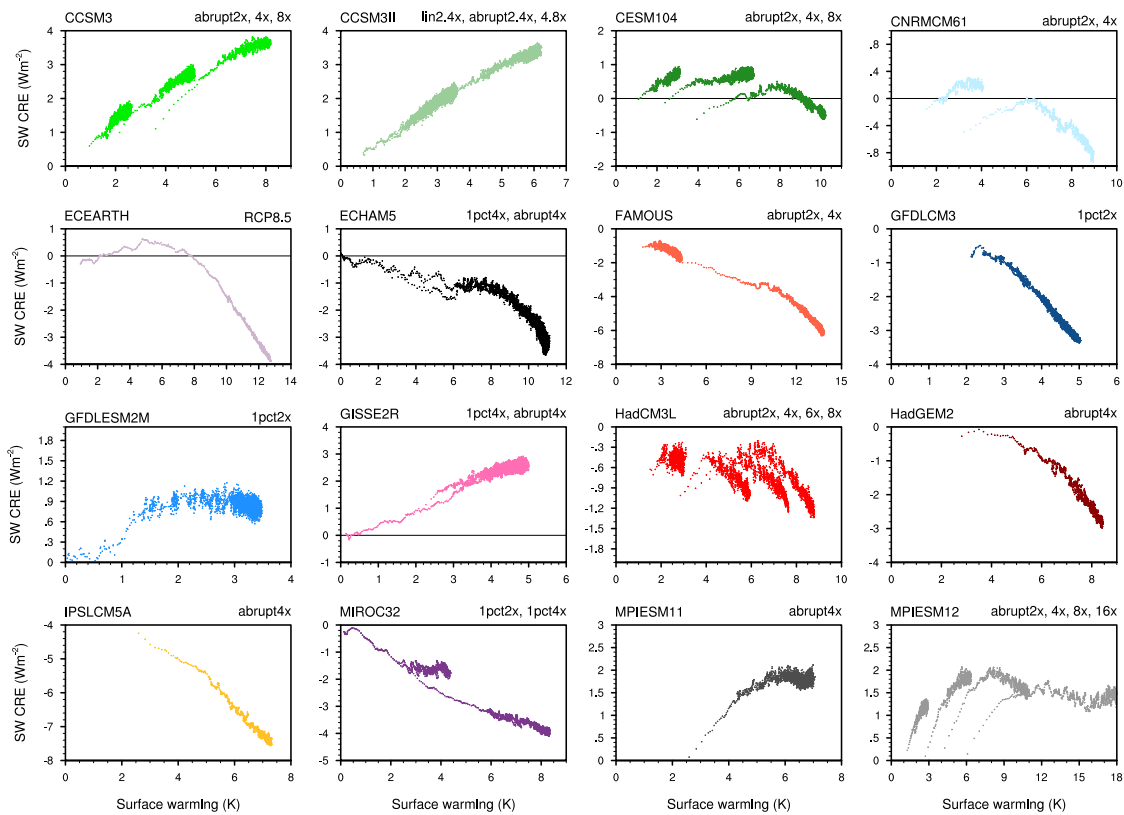
g) Change in temperature anomalies (d)-(c)



895 FIG. 5. Time evolution of the surface air temperature anomaly in the *abrupt4x* simulations. The model mean
896 of CCSM3, CESM104, CNRMCM61, ECHAM5, GISS2R, HadCM3L, HadGEM2, IPSLCM5A, MPIESM11,
897 and MPIESM12 is shown in panel a, b, c, e, and f, while the model mean of only CESM104, GISS2R, and
898 MPIESM11 is shown in panel d and g, due to the length of these contributions. See Table 2 for details of the
899 length of each simulation.



900 FIG. 6. Time evolution of the zonal mean surface air temperature response normalized by the global mean
 901 temperature anomaly. Above (below) 1 means that warming is amplified (reduced) relative to the globally mean
 902 warming (a-d). Panel e-g show the differences (note the difference scale). Panel a, b, e, and f contain only
 903 *abrupt4x* simulations, while panel c, d, and g also contain the *1pct2x* and *RCP8.5+* simulations with integration
 904 lengths above 4000 years. Table 2 lists all simulations and model long names.



905 FIG. 7. Simulated shortwave cloud radiative effects SW CRE for different levels of global surface air tem-
 906 perature changes. Each point is a ten-year running average. Note the different axes labels, which cover a large
 907 range in TOA imbalance and surface temperature. Table 2 lists all simulations and model long names.